Long-term Effects of Altered Foot-Ankle Mechanics on Locomotion Neuromechanics and Energetics

A Dissertation
Presented to
The Academic Faculty

By

Jordyn Schroeder

In Partial Fulfilment
of the Requirements for the Degree
Doctor of Philosophy in the
School of Mechanical Engineering

Georgia Institute of Technology
May 2023

Copyright © 2023 By Jordyn Schroeder

Long-term Effects of Altered Foot-Ankle Mechanics on Locomotion Neuromechanics and Energetics

Approve by:

Dr. Gregory Sawicki
School Of Mechanical Engineering
Georgia Institute of Technology

Dr. Andres Garcia
School Of Mechanical Engineering
Georgia Institute of Technology

Dr. Rudolph Gleason
School Of Mechanical Engineering
Georgia Institute of Technology

Dr. Eni Halilaj
Department of Mechanical Engineering
Carnegie Mellon University

Dr. Adamantios Arampatzis
Department of Sport Sciences
Humboldt-Universität zu Berlin

Date Approved: [April 24th, 2023]

ACKNOWLEDGMENTS

TABLE OF CONTENTS

LIST OF TABLES

LIST OF FIGURES

LIST OF SYMBOLS AND ABBREVIATIONS

MTU   Muscle tendon unit

AMV   Active muscle volume

GAS   Gastrocnemius

SOL   Soleus

EMG   Electromyography

FL   Force-length

FV   Force-velocity

MT   Muscle-tendon

AT   Achilles tendon

CSA   Cross sectional area

Kt   Tendon stiffness

COT   Cost of transport

Pmet   Metabolic power

EMA   Effective mechanical advantage

SUMMARY

Wearable devices that alter foot-ankle mechanics, such as exoskeletons and modified footwear, can change locomotion performance. For example, both passive and powered ankle exoskeletons have been shown to reduce metabolic cost of walking, while high-heeled shoes have been shown to increase metabolic cost. Previous studies provide insights on how foot-ankle devices alter biomechanics and energetics, but the mechanism linking altered foot-ankle biomechanics and whole body metabolic cost remains unclear for human walking. Additionally, little is known about how changes in loading on the biological system over long time periods my impact musculoskeletal structure. These potential changes in structure may lead to altered function over long time scales.

The goal of this thesis was to ask: 1) How do devices that change foot-ankle mechanics alter whole body metabolic cost? 2) Can relatively small changes in musculoskeletal loading over long time scales impact muscle-tendon structural properties? and, 3) How do changes in muscle-tendon structure impact locomotion function? We developed computational and experimental frameworks to investigate how acute and chronic changes to muscle-tendon mechanics impact musculoskeletal structure and whole-body energetic cost of walking.

Through our work, we showed that A) active muscle volume at the ankle can drive whole body metabolic cost of walking (in-vivo), B) the number of steps taken in passive ankle exo-skeletons (in-simulation) and modified shoes with raised heels or raised toes (in-vivo) drives calf muscle-tendon material and morphological adaptation during long-term use of devices (i.e., over months) , and C) chronic changes in calf muscle-tendon properties can profoundly impact locomotion performance (in-vivo).

Taken together, our research pushes fundamental understanding of musculoskeletal structure-function of the human foot-ankle during walking to ecologically relevant long time scales. In doing so, our research also can inform the field of wearable technology offering guiding principles for design, control and/or prescription of long term use based emerging principles of long term neuromechanical adaption of end users.

CHAPTER 1
INTRODUCTION

People continuously adapt how they move over short and long-time scales. Movement, specifically gait, is a complicated interaction between the nervous system and the musculoskeletal system. On short time scale, within minutes, or even step to step, the nervous system continuously adapts its functional motor control strategies to optimize movement [1]–[3]. On longer time scales, muscle and tendon can change structurally, due to various causes like exercise, aging, disuse, or disease [4]–[14]. These changes in structure impact neuromechanics as the nervous system adapts to changes in the musculoskeletal system. It is critical for wearable roboticists to understand how devices the field develops interact with the body on both acute (step-by-step, minutes, hours) and long-term (weeks, months, years) time scales. Structure and function interact across time scales, and external devices can impact neuromechanics and locomotion performance on both acute and long-term time scales.

We are particularly interested in structure-function interaction in the context for the foot-ankle. The calf muscle-tendon unit drives motion as it contributes the majority of the force to propel the body forward during walking and running [15]–[17]. During movement, muscles act like motors, producing forces through a level arm, creating a moment at the ankle and a reaction force to propel the body forward (Fig. 1).
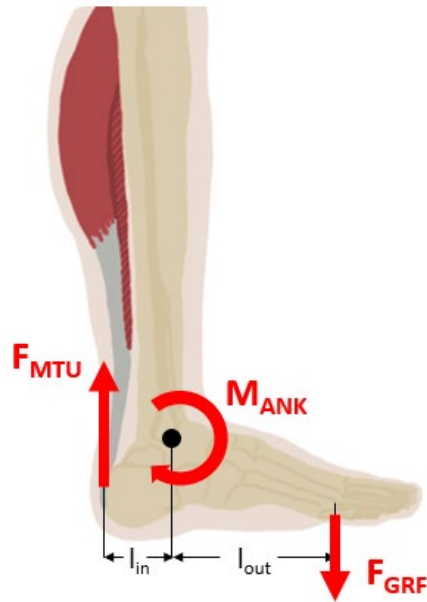
Figure 1. Foot ankle structural free body diagram. F_{MTU} is the force produced by the triceps surae muscle-tendon unit. L_{in} and l_{out} represent the moment arms the relate F_{MTU} to the F_{GRF}, the ground reaction force during walking.

Functionally, the force that skeletal muscles produce depends on muscle dynamics, and fascicle operating points on force-length, and force velocity relationships (Fig. 2). The force length relationship highlights that for an optimal operating length, the largest amount of force can be produced due to the greatest number of actin-myosin cross bridges able to be formed. Shorter operating lengths allow for less cross bridges to be formed, and consequently, the muscle can produce less force. Longer operating lengths, which human do not typically reach in gait, would also produce less force due to less cross bridges forming. In addition to force length relationships, fascicle force velocity relationships dictate how much force a muscle can produce. The faster a muscle shortens during a contraction, the less force it can produce due to less time for cross-bridges to form. Conversely, if a muscle is producing forces while lengthening, i.e.,

lowering a weight, it can produce more force than it could maximally in an isometric condition (Fig. 2).
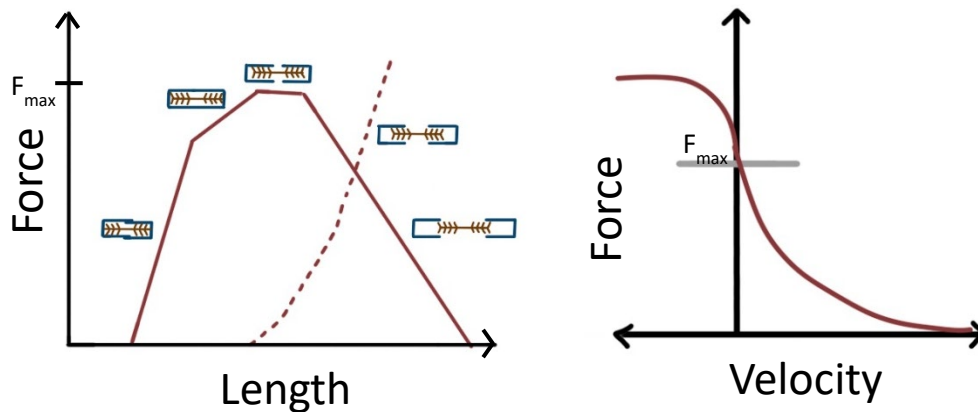
Figure 2. Force-length (left) and force-velocity (right) relationships for skeletal muscles.

Where muscles operate on these force-length and force-velocity curves is driven by both neuromechanics or the activation of the muscles, and the structure of muscle and tendons. The shape of these functional relationships can also change if the muscle or tendon structure changes, i.e., muscle cross-sectional area, length, or tendon stiffness. Additionally, external devices can change foot-ankle mechanics and impact locomotion performance. For example, some running shoes are designed to improve locomotion, while other shoes, like high heels, are designed for aesthetic reasons and can degrade locomotion performance. Ankle exoskeletons are a prime example in the wearables field of devices that impact foot-ankle mechanics and improve walking economy.

In the past decade or so, the wearables field has developed both passive and powered, autonomous and tethered devices that target the hip, knee, or ankle that

3

achieve energy cost reductions [18]. Even passive devices at the ankle have demonstrated energy cost reductions [19] by reducing the force on the biological muscle [20]. While these acute changes in foot-ankle mechanics can achieve locomotion performance benefits, little is known about the impact of these devices on the musculoskeletal system over long-time scales. Additionally, these potential changes in biological structure with long term use can have functional implications that impact locomotion performance of users both during use and after that remove the devices.

There is a critical need to understand structural and functional adaptation to wearable devices in the context of daily use and how they interact long term. These questions are understudied in the field and difficult to address. Long term experiments in-vivo require robust devices, willing participants, and advanced sensing. In this thesis, I combine a computational framework and creative in-vivo experiments to investigate the long-term effects of altered foot-ankle mechanics on locomotion neuromechanics and energetics.

CHAPTER 2
Long-term elastic ankle exoskeleton use need not reduce Achilles tendon stiffness

2.1 Introduction

Lower-limb exoskeleton technology is expanding and has the potential to improve mobility by providing mechanical assistance during human locomotion across a range of settings[21]–[23] . Reducing the metabolic cost of locomotion is a key design objective for these devices [24]and has been achieved using both powered and passive designs[18], [25]–[27]. Exoskeletons that successfully reduce the metabolic cost of locomotion do so by reducing the active muscle volume needed to produce the force and work required to move [28]. These acute metabolic benefits could translate to reduced cost of transport over long-term use and allow people to walk or run farther and faster[18]. On the other hand, chronic unloading of underlying musculoskeletal tissues (*e.g.,* Achilles tendon) could cause atrophy that compromises structural integrity and functional gait performance of the exoskeleton user over long time scales (*i.e.,* week to months to years).

Metabolic energy during locomotion is consumed by active skeletal muscles[29], but series elastic tissues (*e.g.,* tendons) also play a critical role as an energy saving mechanism by storing and releasing energy over each gait cycle. The Achilles tendon (AT), in particular, helps improve economy by taking up a large portion of the overall ankle plantar flexor muscle-tendon (MT) strain, allowing calf muscles to operate at relatively low contractile velocities[30]–[32], reducing the cost of muscle force generation[33]. Interestingly, despite an already effective 'elastic mechanism' operating

in the human plantar flexors, adding supplemental ankle stiffness with an unpowered spring-like exoskeleton can further improve walking economy by 4-7% across a range of speeds[25], [34].

The impact of exoskeleton assistance on muscle energetics is multi-faceted, and acutely influences both users' force demand and force potential[34], [35]. Exoskeletons apply assistive torque about a user's limb-joints that unloads their underlying muscle-tendons (MT) and reduces their biological muscle forces (*i.e.,* reduced force demand). In addition to directly reducing muscle force demand, exoskeletons also impact muscle force potential. That is, because exoskeletons act on the whole MT, they also unload the elastic tissues in series with the muscles (*e.g.,* tendon and aponeurosis). Indeed, through a MT mechanical feedback loop, reduced force (and strain) on in-series tendons acts to shift muscles to longer operating lengths that have improved force economy (*i.e.,* increased force potential)[34]. It is intuitive that exoskeleton-related unloading could lead to atrophy and weakness of musculoskeletal tissues (*e.g.,* similar to space-flight[36], [37]. In addition, because exoskeleton-induced reductions in the metabolic cost of muscle force production depend on the user's MT structural properties, long-term structural changes due to chronic exoskeleton use could reshape the metabolic energy cost landscape itself [38].

Previous work exploring implications of tendon compliance on structure/function relationship on locomotion economy highlight the importance understanding longitudinal exoskeleton impacts [38]. Achilles tendon with optimal properties can minimize muscular energetic costs[39] by elastically deformation allowing muscle fibers to operate at more favorable lengths and velocities[40]. More recent modeling studies have also related tendon compliance to metabolic cost of running[41]. Since both modeling[41] and

6

experimental [38], [40] work has suggested tendon compliance can be optimized for reducing the metabolic cost of bouncing gaits, and because reducing the metabolic cost of locomotion is a (if not the) critical objective for exoskeleton design, understanding tendon remodeling with exo use is tantamount to understanding the long term utility of devices. By not clearly understanding or controlling device impact on tendon compliance, long term implementation of these devices can potentially lead to degraded locomotion economy, negating any intended metabolic benefits

Tendons adapt to their mechanical environments. Experiments in animal models[42] and both *in-vitro* and *in-vivo* [43]–[45] studies in humans over the past two decades indicate that tendon remodels under conditions with increased loading (*e.g.,* intense exercise). These studies found changes in tendon mechanical (*i.e.,* increased stiffness), material (*i.e.,* increased modulus of elasticity), and morphological properties (*i.e.,* increased cross sectional area). On the other hand, tendon atrophy has been observed in chronic unloading, disuse, and aging studies [7], [36], [46]. However, interventions to alter tissue loading can counteract atrophy. For example, in a disuse study, participants on bed rest that completed exercise protocols saw significantly reduced atrophy compared to their non-active counterparts[7]. While exercise and disuse studies provided insight on direction of adaptation, tendon response in the context of nominal locomotion is unclear. Systematic reviews highlight how observed adaptation of asymptomatic, healthy human tendons in increased loading studies is highly variable[47], [48]. A recent meta-analysis found that tendon adaptive responses can be sensitive to several factors including strain magnitude, cycle duration, cycle frequency, intervention duration, and general exercise conditions[47]. These studies highlight that **tendon structure adapts to cyclic loading via a multi-factorial process** and provide

7

a framework for thinking about how long-term exoskeleton use during daily locomotion could impact tendon structure.

Exoskeletons impact both loading on underlying musculoskeletal tissues as well as the user's overall gait. Previous studies of locomotion with elastic ankle exoskeletons used ultrasound to establish that series elastic tissues exhibit lower strain magnitudes in fixed frequency conditions [49]. Intuitively, these lower stain magnitudes should lead to atrophy. However, simply considering acute changes in loading does not acknowledge potential behavioral adaptions that may counteract atrophy. Humans continuously select gait parameters (*e.g.,* speed and step frequency) that minimize metabolic cost of transport[2], [3]. By shifting the metabolic cost landscape, exoskeletons can impact gait parameter selection. For example, if unloading due to exoskeletons reduces metabolic cost, people may choose to move more, increasing total number of steps per day. Increased step count means more loading cycles and hypertrophy of underlying tissues. This highlights a tradeoff between changes in loading, that can decrease tendon strain, and changes in behavior, that can increase cycles.

The purpose of this study was to examine the complicated interaction between *in vivo* mechanical loading (*e.g.,* tendon strain magnitude and rate) and global locomotion behavior (*e.g.,* number of steps per day) during long-term exoskeleton use. Investigating long-term impacts across scale, from tissue level dynamics to gait parameter selection, in real-world environments presents experimental challenges. While recent studies using ultrasound have begun to establish how musculoskeletal tissues change function during short-term bouts of locomotion with research grade exoskeletons[20], [49], there are limits to taking these questions outside of the laboratory. First, exoskeletons are not yet

durable and comfortable enough for long-term daily use. Advances in soft exo-suit technology have enabled users to comfortably operate without maintenance over days, but not weeks. Second, while advances in wearable sensing enable tracking of global parameters like step count and gait speed,[50] there are fewer options for monitoring *in vivo* tissue dynamics outside of the laboratory [51].

Computational modeling can help us get around experimental hurdles[52]. Recently, modeling and simulation has been used to study how passive elastic ankle exoskeletons influence calf muscle-tendon neuromechanics and energetics during acute bouts of steady locomotion [53], [54]. In addition, previous computational studies incorporating mechanobiology of tendons provide insight into both the mechanisms and magnitude of tendon remodeling in response to load [55], [56]. Here, we coupled simple models of muscle tendon unit-level neuromechanics and energetics[53] and tissue-level tendon adaptation [55] to study the long-term impacts of elastic ankle exoskeleton use on Achilles tendon stiffness in silico. We explored a probable range of exoskeleton stiffness under a number of plausible human behavior-driven locomotion paradigms *(i.e.,* constant number of cycles per day, constant distance traveled per day, and constant energy used per day) and estimated how the Achilles tendon would remodel during daily bouts of minimum cost of transport locomotion over a 14-week timescale (=200 days). First, we hypothesized that in the case of a behavioral constraint that maintains a constant, nominal number of locomotion cycles per day, exoskeleton-induced unloading of the Achilles tendon would lead to lower strain magnitudes and atrophy resulting in a new homeostasis at lower tendon stiffness. In addition, we hypothesized that while exoskeleton-induced unloading that decreases Achilles tendon strain (=atrophy) may be unavoidable, lower metabolic cost with exoskeleton assistance would enable a user on a

fixed energy budget to increase the number of locomotion cycles per day (=hypertrophy). Thus, exoskeleton unloading need not upset homeostasis in musculoskeletal tissue properties.

2.2 Methods

Our group previously developed a neuromuscular model of the human ankle plantarflexor muscle-tendon unit comprised of a Hill-type muscle with a series elastic tendon to model the mechanics and energetics of steady bouncing gait, both with and without a passive ankle exoskeleton [53], [57]. This model was adapted to include an aerial phase where the body has no contact with the ground and is only being acted on by gravity. We chose this simplified bouncing gait model because it can capture critical aspects of both tendon and habitual behavioral adaptation through muscle level mechanics as well as well as the mechanical interactions between the exoskeleton, tendon, and muscle. We ran simulations of locomotion with a spring-like exoskeleton over 200 days considering each of three predicted behavioral adaptations to long term device use separately. The exoskeleton stiffness ranged from 0-72 kN/m (0-40% of the starting biological tendon stiffness), representing values that resulted in metabolic costs benefits in human experiments [25] (Fig. 1).
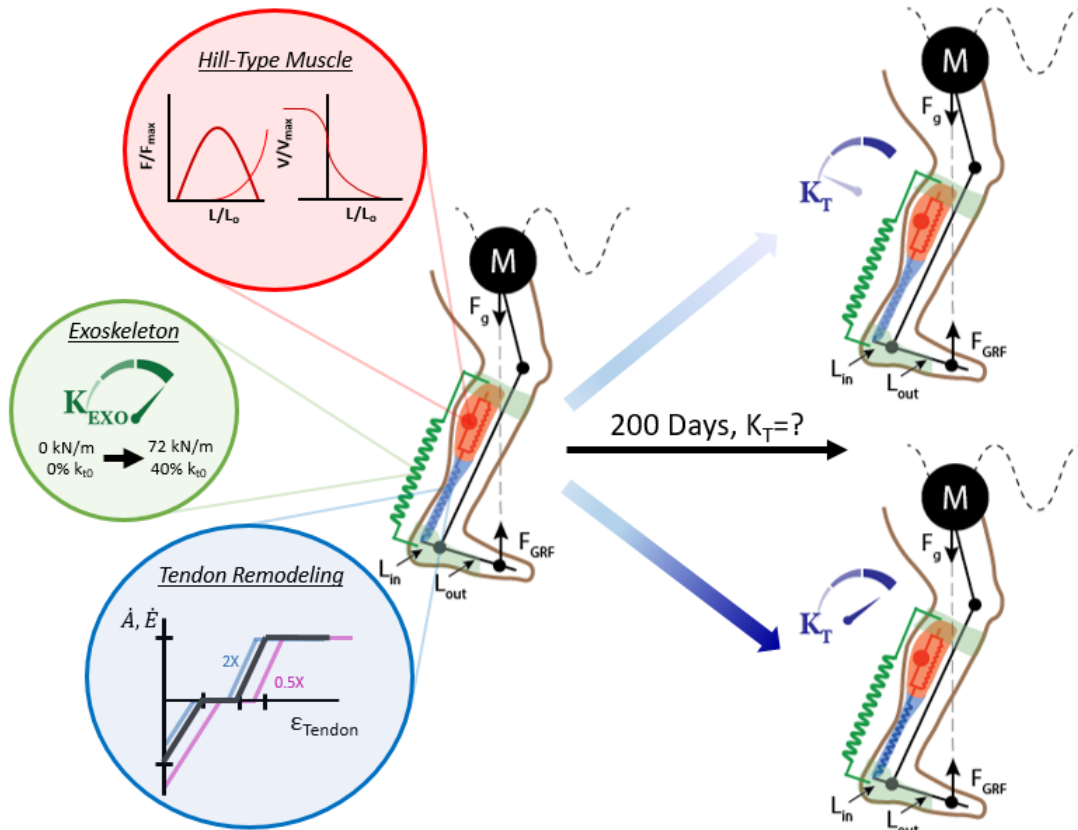
Figure 1: Model overview. The locomotion model is comprised of a Hill-type muscle model of ankle plantar-flexors with a series-elastic tendon element with stiffness k_T. The tendon is subject to mechanobiological adaptation on a day to day basis that depends on the strain per cycle and number of cycles per day. A passive exoskeleton is modeled by a spring in parallel with the plantar-flexors that has stiffness k_{EXO}. Change in tendon stiffness is tracked over a 200 day period.

Within the simulation of each day, we proceeded as follows (Fig. 2):

(i)   Given current tendon stiffness at the start of the day and exoskeleton stiffness, we swept applicable muscle stimulation frequencies [2.2-3.5Hz][58] and activations [10-100%] to find the stimulation-activation combination that minimized the metabolic cost of transport and then fed these parameters into the next daily locomotion run. We defined cost of transport (CoT) as follows:

$$CoT = \frac{\bar{P}_{met}}{f * HH}$$ (1)

Where f is the muscle stimulation frequency, HH is hop height, and $\bar{P}_{met}$ as defined in (Eq. 2) is dependent on muscle velocity and activation. Conditions with no aerial phase or injury risk due to peak muscle strain of greater than 30%[59], [60] were excluded. This simulated an adaptation in habitual gait parameters to long term exoskeleton use based on previous work that shows humans optimize gait parameters to minimize cost of transport during cyclic locomotion [61]–[65] and while wearing ankle exoskeletons[2], [3].

(ii)   Using the selected gait parameters, we simulated steady-state cyclic locomotion using a neuromuscular model with a passive ankle exoskeleton. Initial model parameters can be seen in (Table 1). Metabolic cost was calculated using the following equation [53]:

$$\bar{P}_{met} = \frac{1}{T_{stim}} F_{max} v_{max} \int_{t=0}^{T_{stim}} [\alpha(t) P_{met}\left(\frac{v}{v_{max}}\right)] dt$$ (2)

Where $\bar{P}_{met}$ is average metabolic rate, T_{stim} is cycle period, F_{max} is maximum force produced during an isometric contraction, v_{max} is the maximum unloading rate of shortening, $\alpha(t)$ is muscle activation, and $P_{met}\left(\frac{v}{v_{max}}\right)$ is a dimensionless metabolic cost at time t calculated from [66] as follows:

$$P_{met}\left(\frac{v}{v_{max}}\right) = F_{max} v_{max} \phi(\frac{v}{v_{max}})$$ (3)

$$For\ v > 0: \phi\left(\frac{v}{v_{max}}\right) = 0.1 - 0.11\left(\frac{v}{v_{max}}\right) + 0.06e^{23\left(\frac{v}{v_{max}}\right)} \qquad (4)$$

$$For\ 0 < v < v_{max}: \phi\left(\frac{v}{v_{max}}\right) = 0.23 - 0.16e^{-8\left(\frac{v}{v_{max}}\right)} \qquad (5)$$

Next, we determined the number of locomotion cycles per day using one of three behavioral criteria:

1) *Energy Budget:* Maintaining total energy (103 kJ) use per day

2) *Distance Budget*: Maintaining total distance (319 m) traveled per day

3) *Cycle Budget*: Maintaining a nominal 5,000 cycles per day [67]

Hop height, HH, was calculated as maximum center of mass position during steady-state locomotion and used to represent distance covered in a cycle. Both energy budget and distance budget were calculated using a nominal condition of no exoskeleton for the nominal cycles per day (5,000 cycles).

Total number of cycles and peak tendon strain were fed into the tendon mechanobiological relationship. Peak tendon strain, ε_{Tendon}, was calculated as:

$$\varepsilon_{Tendon} = \frac{l}{l_o} \qquad (6)$$

Where l is the peak tendon length during a steady state cycle, and l_o is the resting length of the tendon.

Table 1: Ankle plantarflexor muscle-tendon model initial parameters

Model Parameters

k_{t0}	180 kN/m
F_{mus_max}	6000 N
L_{ten_slack}	0.237 m
L_{mus_0}	0.055 m
V_{mus_max}	0.45 m/s
T_{act}	0.0329 s
T_{deact}	0.0905 s
EMA	0.33

(iii)   The number of locomotion cycles and tendon strain on a given day are inputs to a model of the mechanobiological adaption of tendon cross section area (A) and Young's modulus (E), adapted from [55]. This relationship considers peak tendon strain as the driver of mechanobiological adaptation with negative values for $\dot{A}$ and $\dot{E}$ at low strain, no change in a 'dead band' at intermediate strains, and positive values at high strains.

These strain values were scaled to have at nominal locomotion (hopping) with no exoskeleton in the center of the 'dead band' (Fig. 3). While other studies suggest that high strains lead to tendon degradation, these strains fall outside of physiological values and led to rupture [68]. Additionally, exercise studies support our proposed mechanobiological relationship as they saw

tendon homeostasis at mid-level strains and hypertrophy at high level strains [43], [69].

Despite a wealth of available data from controlled exercise studies, there remains a clear need to investigate how tendon adapts under conditions that better represent in vivo loading cycles during locomotion. Exercise and disuse studies provide insight on the range of magnitude of tendon hypertrophy and atrophy [9], [43], [69]–[72], as well as a general adaptation timeline. However, these studies do not provide a clear indication of how sensitive tendon adaptation is to changes in number of cycles, especially in the context of daily locomotion. To model the impact of cycles on the tendon mechanobiological relationship, we used a sigmoid function to create a family of tendon stiffness adaptation curves as a function of cycles per day (Supplemental Figure 2). Specifically, with greater cycles per day from nominal (i.e. >5,000 cycles per day), the tendon stiffness-strain relationship is shifted leftward, resulting in atrophy, homeostasis, and hypertrophy strain limits to be lower. Conversely, with fewer number of cycles per day than nominal (i.e. <5,000 cycles per day), a rightward shift was used. A sensitivity analysis was performed to establish bounds on this sigmoid function that constrained results to physiologically feasible adaptation magnitudes and timeframes (Supplemental Figure 3-4).

Updated A and E values are used to find tendon stiffness (k_{Ti}) at the start of a given day using the following relationship:

$$k_{Ti} = \frac{E_i A_i}{l_o} \qquad (6)$$

Where E_i is current Young's modulus at the start of a given day and A_i is current cross sectional area at the start of a given day. The updated tendon stiffness is used for the next modeling day.
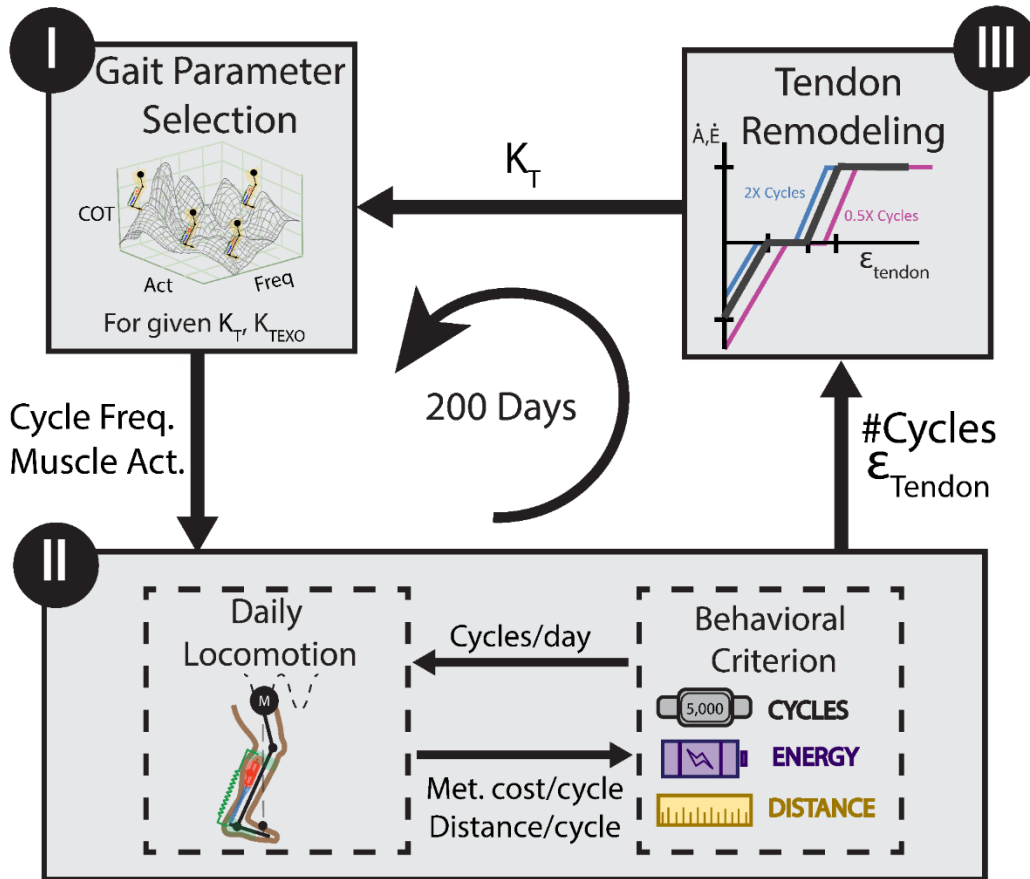
Figure 2: Model computational flow. For 200 simulated days, model flow per day is as follows: I) Given current tendon stiffness, model parameters (frequency and muscle activation), are determined by minimizing cost of transport. II) Daily locomotion is simulated using a neuromuscular model with a passive ankle exoskeletons. Number of cycles per day is determined by one of three behavioral criterion: a) constant cycles per day b) constant energy used per day or c) constant distance traveled per day. III) Tendon mechanobiological adaptation, driven by tendon strain and locomotion cycles, is used to update tendon stiffness
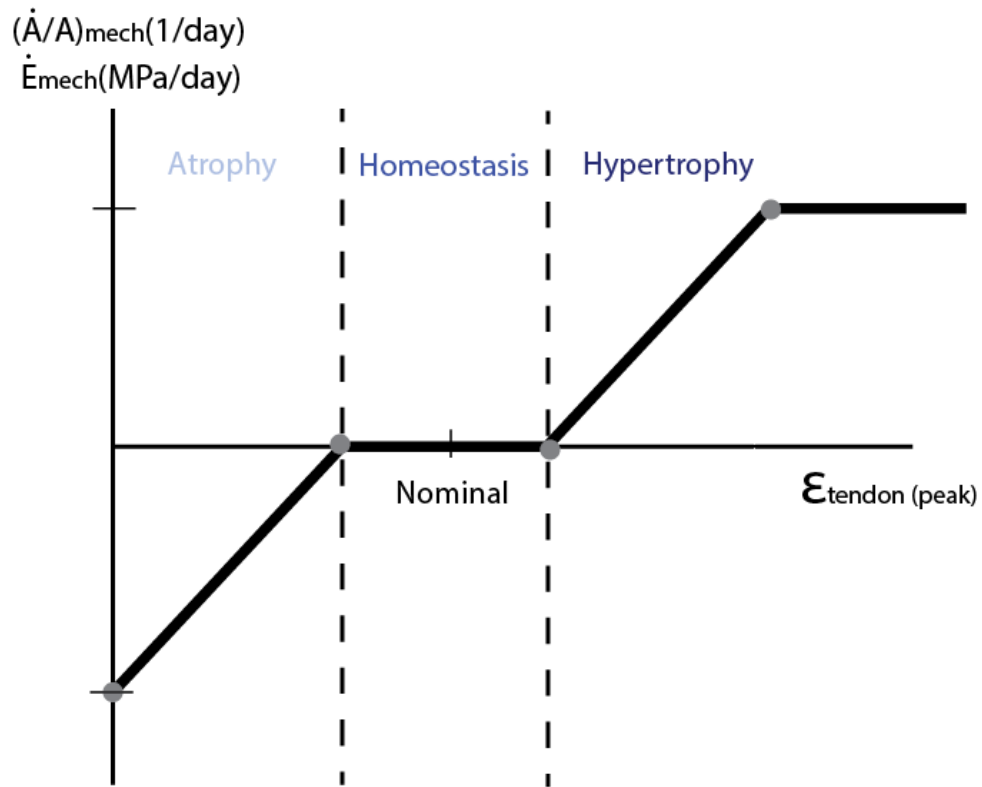
Figure 3: Mechanobiological adaptation. The piece-wise linear relationship governing tendon mechanobiological adaptation from [55] We set tendon strain ($\varepsilon_{tendon\ (peak)}$) in the mid-zone of homeostasis to 9.2% in order to match the value observed during the baseline locomotion condition in this study. Then, by scaling the values in [55], we set atrophy to occur until 7.1% strain and hypertrophy to begin at 12.2% strain. $\dot{A}_{max}/A$ and $\dot{E}_{max}$ are set to 0.01 d^{-1} and 5 MPa d^{-1} respectively [55] This relationship shown holds for a nominal number of cycles and is shifted when daily cycles are shifted from nominal (Supplemental Figure 2-4).

We also ran additional simulations holding cycles constant throughout the 200 simulated days. These 'prescribed' number of cycles ranged from 0.5X nominal (2,500 cycles) to 2X nominal (10,000 cycles)

2.3 Results

2.3.1 Locomotion mechanics and energetics

Sample outputs of daily locomotion for an intermediate exoskeleton stiffness (k_{EXO}=54 kN/m) with tendon stiffness of 90%, 100%, and 110% of the starting k_T suggest stable, cyclic hopping for a range of tendon stiffness values (Fig. 4). During this example motion, ground reaction forces and hop height decreased as tendon compliance increased. The opposite trend was seen for tendon strain and muscle operating length. Whole ankle positive mechanical power as well as metabolic cost in these trials compared to that of both modeling[53], [57] and single leg hopping in a previous human study[49].
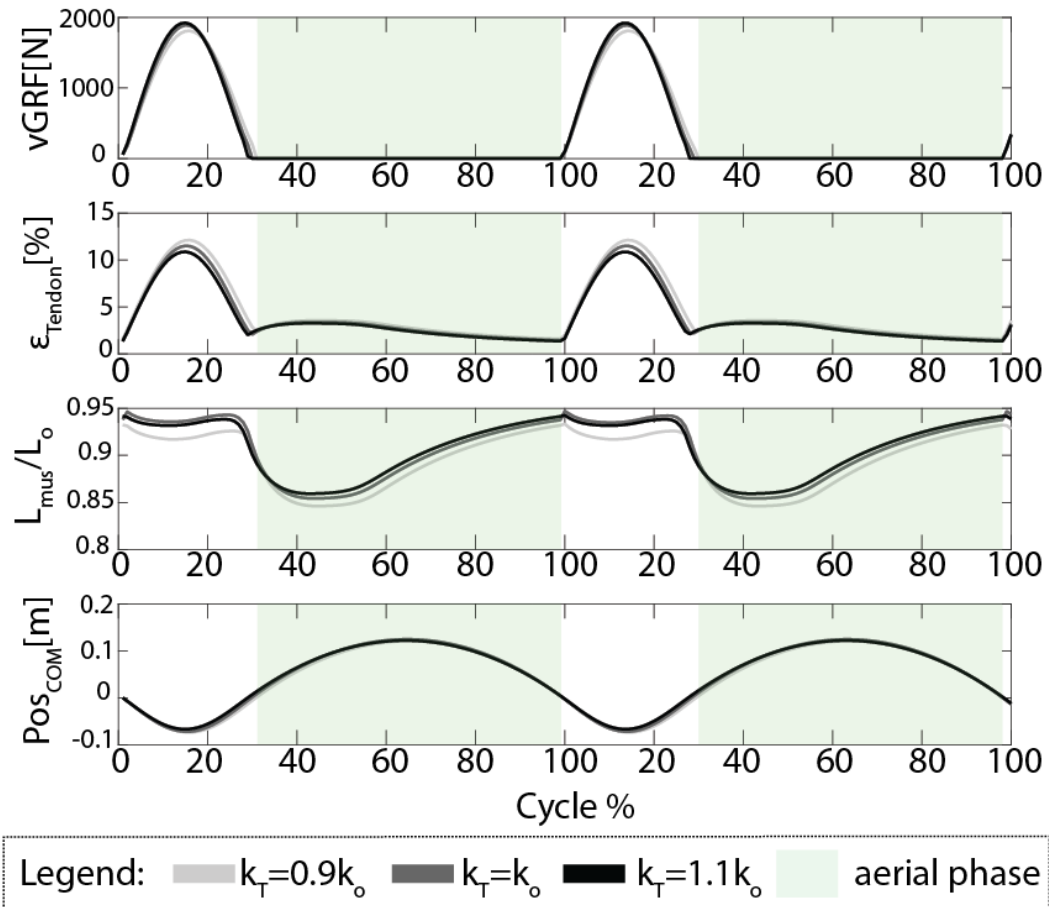
Figure 4: Muscle-tendon mechanics. Vertical ground reaction forces, tendon strain, normalized length of muscle and position of center of mass for a moderately stiff exoskeleton (54 kN/m) for a tendon that is 90% of nominal starting stiffness (light grey), nominal tendon stiffness (dark grey), and 110% of nominal starting stiffness (black). Aerial phase is shown in green, and ground contact phase is shown in white. The frequency and activation were selected to minimize cost of transport for each give tendon stiffness. The selected frequencies were 2.2Hz, 2.2Hz, 2.25Hz and selected activations were 79%, 83%, 90% MVC for $k_T = 0.9k_0$, k_0 and $1.1k_0$ respectively.

2.3.2   Tendon stiffness adaptation for constrained simulations

Energy constraint:

Tendon adaptation over 200 days for the energy constraint behavioral paradigm resulted in no change in tendon stiffness for all k_{EXO} values (Fig. 5). Average energy per day was constrained and was therefore constant throughout all model runs (103 kJ). Average distance per day increased compared to nominal locomotion (i.e. 5,000 cycles/day and 319 meters/day) without an exoskeleton (Table 2). Within this behavior, exoskeletons both increased and decreased tendon stiffness and increased cycles for most time series points (individual days), leading to overall tendon stiffness homeostasis (Fig. 6a).

Distance constraint:

For the distance constraint, no changes in k_T were seen for the condition without an exoskeleton and all other k_{EXO} values resulted in decreased tendon stiffness (Fig. 5). Within fixed distance trials, a bowl shape with the greatest losses in tendon stiffness at intermediate exoskeleton stiffness values occurred (Fig. 5b). Average energy per day decreased as exoskeleton stiffness increased and average cycles followed a bowl shape with decreased cycles for intermediate exoskeleton stiffness values. Distance per day was constrained and stayed the same for all trials (Table 2). Within this behavior,

19

exoskeletons increased tendon strain and decreased cycles per day for most time series points (individual days), leading to overall stiffness decreases (Fig. 6a).

Cycle constraint:

For the constant cycles per day constraint, all conditions resulted in tendon homeostasis, where there was no change in tendon stiffness (Fig. 5). Average energy per day decreased as exoskeleton stiffness increased, and opposite trends were seen in distance per day. Cycles were constant, and held at nominal (5,000) for all conditions (Table 2). Parameters that minimized cost of transport resulted in locomotion with strains within +/-10% of the nominal strain (Fig. 6a).

Table 2: Modeling results after 200 simulated days of locomotion, sweeping exoskeleton stiffness values for each behavioral criterion

	Behavioral Criterion		
	Energy	Distance	Cycles
Δkt [%]			
kexo [kN/m]			
0	0	0	0
18	0	-21.38	0
36	0	-28.03	0
54	0	-28.35	0
72	0	-8.86	0
Avg. Energy [kJ day^{-1}]			
kexo [kN/m]			
0	103	103	103
18	103	63	107
36	103	55	100
54	103	47	94
72	103	42	88
Avg. Cycles [day^{-1}]			
kexo [kN/m]			
0	5000	5000	5000
18	4847	2975	5000
36	5192	2913	5000
54	5507	4104	5000
72	5889	5049	5000
Avg. Distance [m day^{-1}]			
kexo [kN/m]			
0	319	319	319
18	559	319	576
36	626	319	603
54	685	319	622
72	742	319	630
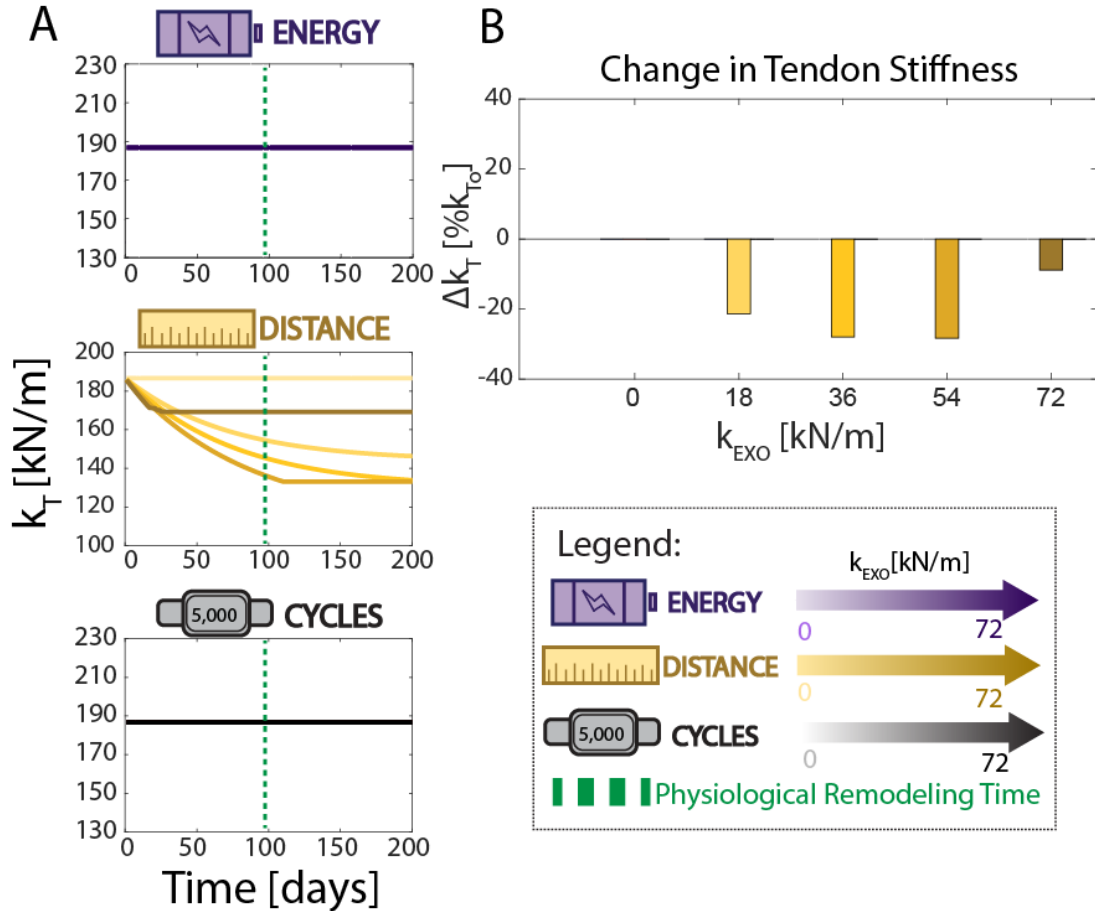
Figure 5: Tendon stiffness adaptation. A) Time series of tendon stiffness (k_T) for each exoskeleton stiffness value (k_{EXO}=0-72 kN/m) for three locomotion behavioral criterion. Physiological remodeling timeframe (~14 weeks) is indicated by the green dashed line. **B)** Percent change in tendon stiffness (Δk_T) for each exoskeleton stiffness, k_{EXO}.

2.3.3 'Prescribed' cycles around nominal:

As described previously, constraining cycles to nominal resulted in no change in tendon stiffness for all exoskeleton values. However, constraining cycles from 0.5X nominal to 2X nominal, resulted in tendon stiffness decreases, homeostasis, and increases (Supplemental Figure 1). Individual time series points (individual days), for all

'prescribed' cycle simulations show that increases in tendon stiffness occur for simulated days with increased cycles and get larger as tendon strain increases (Fig. 6b). For days with decreased cycles, most simulations resulted in decreased tendon stiffness that lessened as tendon strain increased (Fig. 6b). For exoskeleton values 0, 18, 36, 54 and 72 kN/m, there are a range of prescribed cycles that results in decreased tendon stiffness, a range that result in homeostasis, and a range that result in increased tendon stiffness (Fig. 7). For a exoskeleton with a high stiffness of 90 kN/m, all no values of prescribed cycles resulted in tissue gains (Fig. 7).
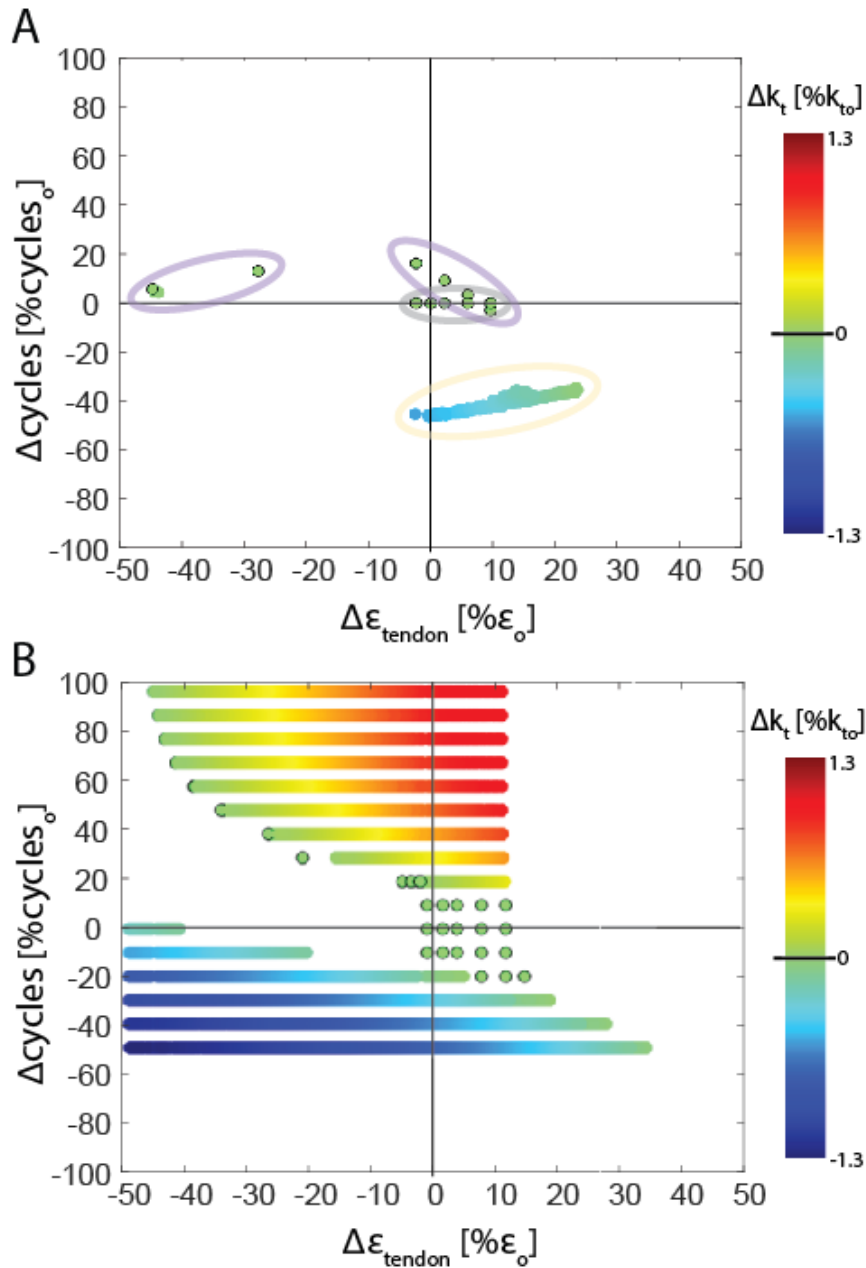
Figure 6: Factors driving tendon remodeling. Percent change in tendon stiffness (Δk_T), number of locomotion cycles (Δcycles), and peak tendon strain ($\Delta\varepsilon_{tendon}$) for each simulated day over the 200 day simulation period. Clusters are grouped by locomotion behavioral criterion: constant energy (violet), constant distance (amber) and constant cycles (grey). B) Percent change in tendon stiffness, number of cycles and tendon strain for all simulated days holding cycles constant from 0.5X nominal to 2X nominal. Conditions with large increases in tendon stiffness over time (red circles) were associated with increased number of cycles that in some cases offset significant reductions in tendon strain.
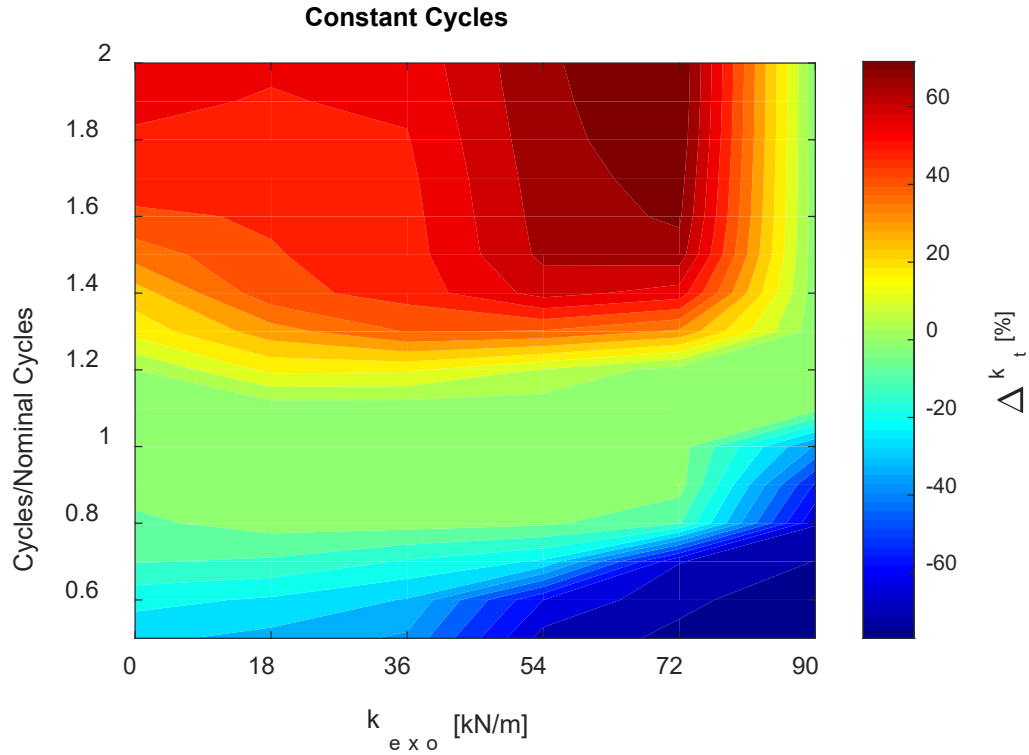
Figure 7: Constraining Constant Cycles Percent change in tendon stiffness (Δk_T), for each exoskeleton stiffness with cycles held constant from 0.5X nominal to 2X nominal for 200 days. Warm colors indicate increases in tendon stiffness, green indicates homeostasis, and cool colors indicate decreases in tendon stiffness.

2.4 Discussion

The purpose of this modeling study was to investigate impacts of long-term elastic

exoskeleton use on a user's Achilles tendon stiffness. Over a simulated 200 day period,

for exoskeletons across a range of stiffness values, we examined how the most

economical locomotion cycle (i.e., hop frequency and height) impacted tendon tissue

remodeling under various behavioral criterion constraining the number of locomotion

cycles per day. Surprisingly, we found no observed changes in tendon stiffness for both

the constant nominal cycles and constant energy criterion at all exoskeleton stiffnesses

(Fig. 5). For the constant distance constraint, we observed a decrease in tendon stiffness of 21.38%, 28.03%, 28.35%, and 8.86% for exoskeletons with stiffness values of 10%, 20%, 30%, and 40% of the starting biological tendon stiffness respectively, indicating a 'sweet spot' for exoskeleton parameters if humans constrain behavior by distanced traveled. As expected, modulating the number of cycles at 0.5X to 2X led to a range of adaptation from atrophy to hypertrophy. For all conditions, most results fell within the physiological ranges of Achilles tendon remodeling time and magnitude of stiffness changes observed during both unloading and intense exercise protocols, giving us confidence in our modeling approach.

We hypothesized that the constant nominal cycle constraint would lead to reduced tendon strain and atrophy, however we observed increased tendon strain for many conditions and all conditions resulted in no change in tendon stiffness (Fig. 6A). The unexpected increases in strain occurred because of the combination of hop frequency and muscle activation that were selected for those exoskeleton conditions to minimize cost of transport. Despite the exoskeleton changing tendon strain +/-10% of nominal, the observed tendon stiffness homeostasis can be attributed to the shape of the tendon mechanobiological relationship where homeostasis is maintained for a range of strains around nominal (Fig. 3). This suggests that exoskeletons may not change tendon strain enough to have musculoskeletal impacts if a nominal number of cycles is maintained while wearing the devices. A hopping study in humans observed that change in length of the series elastic element were not different with an exoskeleton, despite an observed reduction in soleus force, which they speculated to be from tendons operating in the toe region of their force-length relationship [58]. This, in combination with our observed changes in tendon strain highlight the need to further investigate muscle-tendon

dynamics with exoskeletons, specifically in walking, when humans are not constrained to specific gait parameters (step frequency, speed, etc.).

We also hypothesized that if a predicted behavioral adaptation increased the number of locomotion cycles per day, this could compensate for unloading caused by the exoskeleton and that tendon stiffness would not necessarily decrease over time despite exoskeleton use. We found that tendon strain was indeed not the sole driver of tendon adaptation and that the number of daily cycles, as determined by a given behavioral paradigm, also drove remodeling (Fig. 6). For the energy constraint criterion, despite some decrease in tendon strain, there was no change in tendon stiffness due to the increase in daily cycles from nominal, supporting our hypothesis (Fig. 6A). These results indicate that for long-term lower-limb exoskeleton users on a strict energy budget, a new homeostasis emerges whereby reduced loading in musculoskeletal structures is naturally offset by more, less costly gait cycles per day. On the other hand, the constant distance constraint led to decreased tendon stiffness, despite most simulations resulting in increased tendon strain. Though the hop frequency and muscle activations that the model selected increased tendon strain, these parameters also led to higher hops, resulting in less cycles required to move the same distance. The observed decrease in tendon strain for the constant distance constraint was less for simulations with higher number of cycles (Fig. 6A). So, although increased cycles compensated for unloading in the constant energy criteria, the atrophy observed in the constant distance criterion highlights the need to investigate how human's habitual behavior changes with long term exoskeleton use.

When we held cycles constant, sweeping values from 0.5X to 2X nominal, the tradeoff between strain and number of cycles is further highlighted (Fig. 6B). Conditions with decreased strain but increased cycles resulted in homeostasis or an increase in tendon

stiffness. On the other hand, conditions with increased strain but decreased cycles resulted in homeostasis or a decrease in tendon stiffness. As expected, conditions with decreased strain and cycles primarily resulted in decreased tendon stiffness, and conditions with increased strain and cycles resulted in increased tendon stiffness (Fig. 6B). 'Prescribing' constant cycles revealed the landscape of changing tendon stiffness for each exoskeleton stiffness value (Fig. 7). Relevant stiffness values of the exoskeleton (0-72 kN/m) resulted in atrophy, homeostasis and hypertrophy for low, medium (near nominal=5000 cycles/day) and high number of locomotion cycles per day respectively. Even for a very stiff exoskeleton (90kN/m) a high number of cycles could overcome atrophy that was simulated to occur at and below nominal cycles. An understanding of this landscape and time series (Supplemental Fig.1) indicates the potential to modulate tendon stiffness with control of exoskeleton stiffness and number of cycles.

This model captures important physiological characteristics in-silico and can provide insight on how global behavior and exoskeleton parameters can impact tendon adaptation. While this work can be used to generate hypotheses for future human experiments, there are important limitations. We used a hopping model because there is readily available results from both modeling and human experiments [31], [53], [57], [73]–[75] of spring exoskeleton-assisted hopping to compare. We also considered just the ankle joint since a majority of limb total positive mechanical power during hopping comes from this single joint [76]. Future studies could implement a more complicated, multi-joint walking model. We also simplified human behavioral adaptation to long term device use into three distinct categories. It is possible that humans use a combination of these three or others that we did not consider. Further studies on human neuromechanical adaptation to device use outside of the laboratory are necessary.

For our tendon biomechanical adaptation relationship, we scaled increased strains in this task to map results onto cross-sectional area and modulus response to mechanical loading used in previous studies. While it is unclear if results directly compare to behaviors with lower strain rate [43], [68], [69], [77], we expect general behavior to follow a similar pattern. Because it is not clearly known how tendon adaptation is impacted by cycles, we chose to shift the relationship left for increased cycles, which lowers the trigger points for tendon homeostasis and hypertrophy, and the opposite for decreased cycles. Other cyclic effects on the adaptation relationship could be scaled remodeling rate of change or range of the homeostasis strain region. The amount trigger points shifted was considered in a sensitivity analysis where we defined ranges of physiologically relevant changes in stiffness to be no more than 25% increases or 30% loss in a 200-day period. Because tendon response to chronic mechanical loading varies depending on study specific parameters [45], [47] and no study has been done to match our loading paradigm, these ranges could be different. However, changing sensitivity did not result in changes in general loading behavior. We also chose a sensitivity where most exoskeleton stiffness values resulted in homeostasis within 14 weeks, which is the typical time frame which tendon adaptation occurs in exercise studies [9], [43]–[45], [70]. Finally, muscle properties in our modeling were held constant. Though we acknowledge that both muscle and tendon can be impacted by changes in loading and cycles, we anticipate that tendon and muscle would follow the same remodeling behavior. For example, cases with tendon atrophy would also result in muscle atrophy. Future studies could account for muscle adaptation by allowing maximum force, maximum velocity, physiological cross-sectional area and muscle slack length to change with loading patterns and cycles.

Despite the simplicity of this model, we were able to generate steady-state cyclic movements comparable to human spring assisted hopping experiments mechanically and energetically. Appropriate muscle-tendon unit mechanics allowed us to explore tendon loading under varied gait and exoskeleton parameters. Using a sensitivity analysis for cyclic impact on the tendon mechanobiological adaptation relationship enabled us to constrain results to physiological values for both magnitude and duration of tendon remodeling. Our results highlight the importance of further investigating loading conditions and cyclic impact on remodeling, especially during daily activities. While exercise and unloading studies provide critical information about tendon remolding, they do not fully capture conditions that reflect real world settings. Studies implementing wearable devices can use exoskeletons as a function to 'tune the dial' on tendon loading in the context of normal human locomotion. This can provide a platform to further investigate tendon response to longitudinal mechanical loading and unloading during daily tasks. Expanded understanding of tissue response to varied loading and cycles in vivo can be used to improve model predictions of both rate and magnitude of remodeling.

Our modeling and simulation results indicate that people may be able to get short- and long-term benefits from exoskeletons without atrophy, and have major implications for device design and control for real world settings. Beyond highlighting the need to consider loading paradigm and changes in gait parameter selection, our results suggest that modifying human locomotion behavior in conjunction with device parameters can enable regulation of tissue remodeling. We can modify human behavior through feedback from a step counter or more advanced sensors. Device design can also consider loading on the musculoskeletal system. An advanced approach could involve considering tendon stiffness and cost of transport in a controller objective function with a

30

powered device that can control exoskeleton assistance based on a person's level of activity. Not only is there potential to mitigate tissue atrophy for healthy populations and still reap metabolic benefits of from exoskeletons, but there is also potential for advanced exoskeleton systems to steer tissue properties during daily activities in order to maintain long-term musculoskeletal health. This has specific applications for healthy, rehabilitative, and aging populations.

2.5 Supplementary Material

Supplementary Figure 1 shows time series of tendon stiffness (k_t) for each 'prescribed' constant cycle value from 0.5X nominal to 2X nominal for exoskeleton stiffness (k_{exo}) values from 0-90 kN/m. Supplementary Figures 2-4 detail the sensitivity of our tendon stiffness (k_t) vs. time results across exoskeleton stiffness (k_{exo}) conditions for a range of parameters shaping the non-linear tendon remodelling relationship adapted from Wren et al. [55]
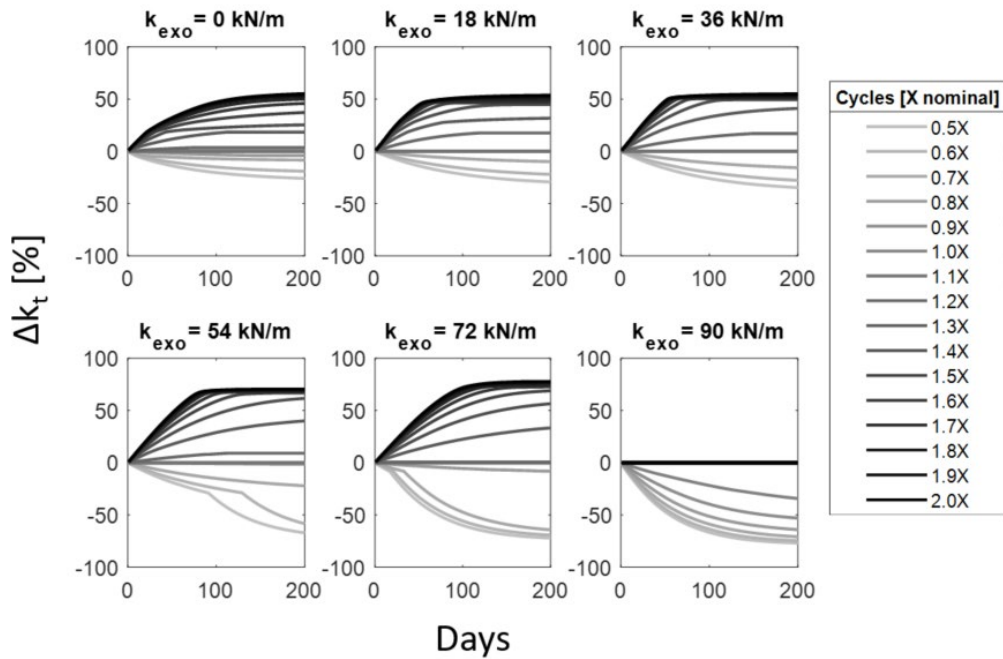
Supplemental Figure 1: Constant Cycles Time Series Time series of tendon stiffness for each simulated exoskeleton stiffness value with cycles held constant from 0.5X nominal to 2X nominal for 200 days.
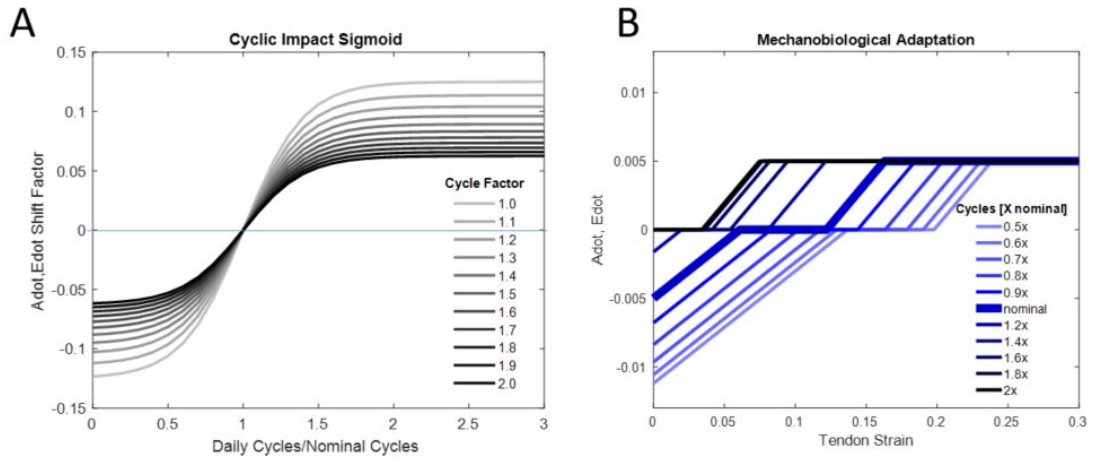
Supplementary Figure 2: A) Sigmoid function used to shift the tendon mechanobiological adaptation relationship in Figure 3 to account for increases/decreases from the nominal 5,000 locomotion cycles per day. Various cycle factors, i.e. how sensitive remodeling is to number of cycles are shown. **B)** Impact of changing number of locomotion cycles on the tendon mechanobiological adaptation relationship using the sigmoid function for cycle factor 1.4 in A. Increasing/decreasing the number of locomotion cycles shifts the tendon strain for homeostasis to lower/higher values, respectively. The cycles factor that we used in our study (nominal=1.4) was chosen to match expectation for the magnitude and time course of tendon adaption based on the literature[43], [44], [72]. More details on this choice and the sensitivity of our results to changes in the cycles factor value are shown in Supplementary Figure 2 (for impact on changes in tendon stiffness over time) and Supplementary Figure 3 (for impact on number of days to steady-state tendon stiffness).
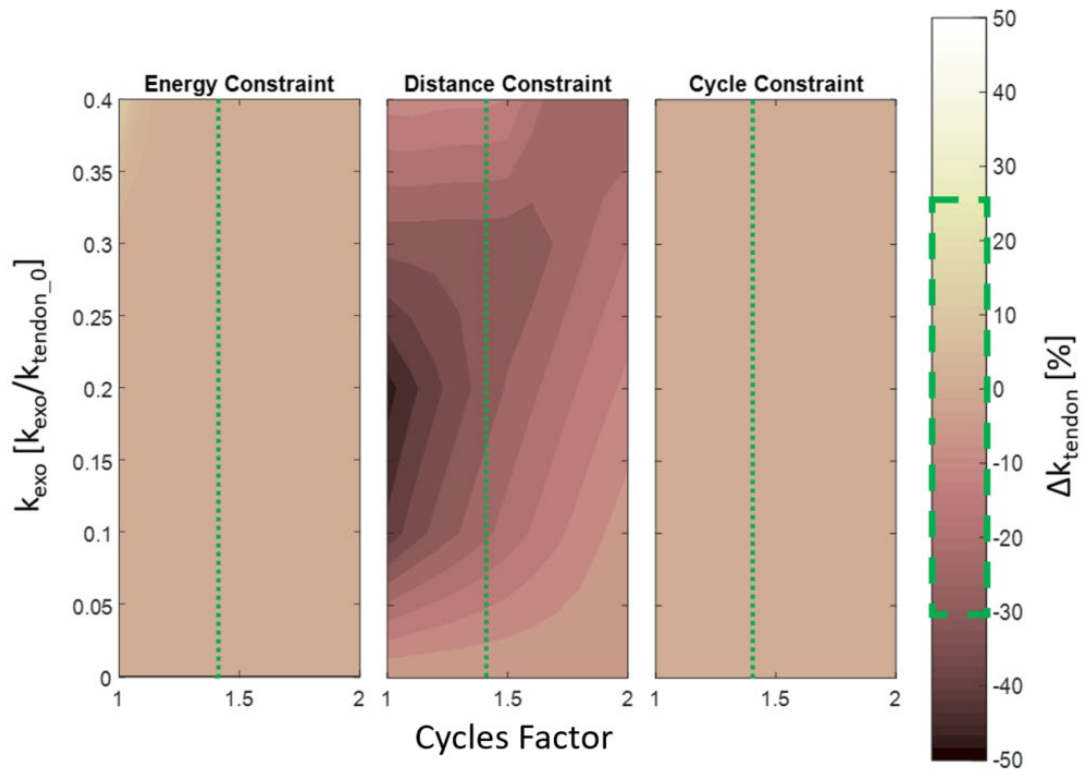
Supplementary Figure 3: Sensitivity of the change in tendon stiffness over time to locomotion cycle-dependent differences in the tendon mechanobiological adaptation relationship. Cycles factor (range: 1-2) and exoskeleton stiffness (range: 0-0.4 times k_T at day zero) values were swept with the magnitude of change in tendon stiffness after 200 days (Δk_T) as the outcome. Based on studies of exercise induced changes in tendon stiffness [69], we expected changes in tendon stiffness (brown shading) between -30%-+25% (dotted green outline on brown color map). The cycles factor that we used in our study (=1.4, green dotted vertical line) generated changes in tendon stiffness within the expected physiological range across all exoskeleton stiffness values for each of the three behavioral criterion.
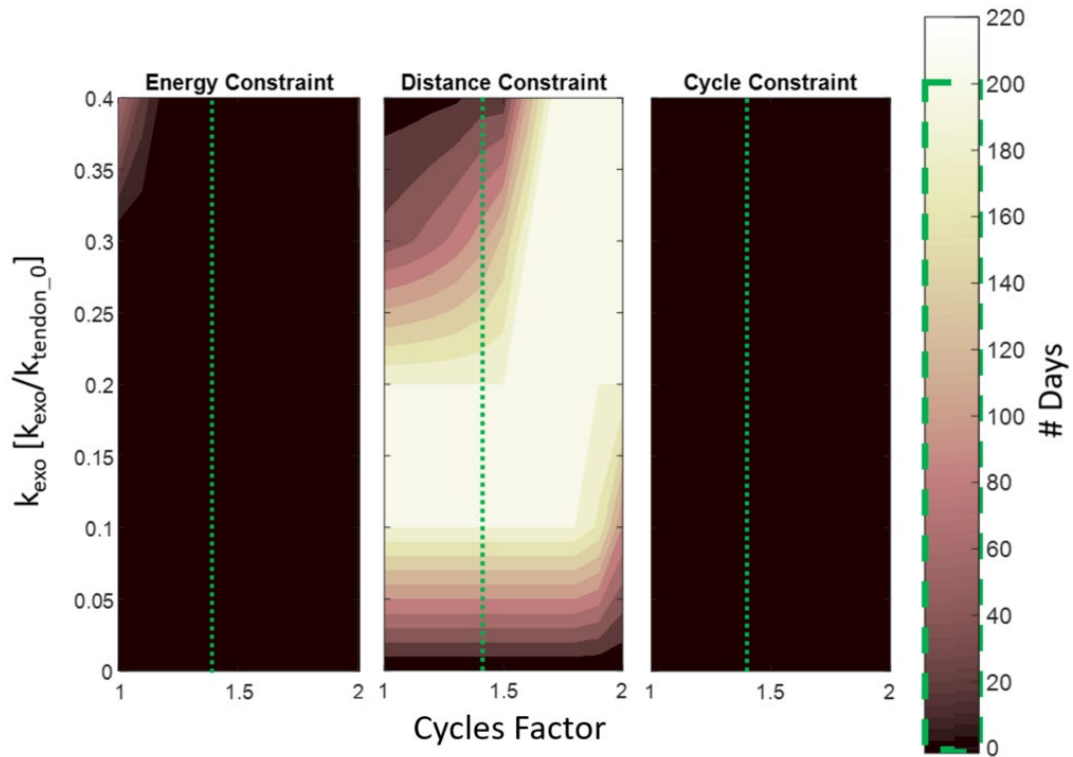
Supplementary Figure 4: Sensitivity of the time to steady-state tendon stiffness to locomotion cycle-dependent differences in the tendon mechanobiological adaptation relationship. Cycles factor (range: 1-2) and exoskeleton stiffness (range: 0-0.4 times k_T at day zero) values were swept with number of days to steady-state tendon stiffness as the outcome. Targeted range of physiological adaptation time of 0-200 days is indicated on the heat map legend (green outline on brown color map). The cycles factor that we used in our study (=1.4, green dotted vertical line) has values that fall within the acceptable range for most exoskeleton stiffness values for all three behavioral criterion.

CHAPTER 3
Acute Changes in Foot-Ankle Mechanics Impact Whole Body Metabolic Cost of Walking

3.1 Introduction

Wearable devices that alter foot-ankle mechanics can change locomotion performance. For example, both passive[19] and powered[18], [26], [27], [78] ankle exoskeletons have been shown to reduce whole body energy consumption. On the other hand, shoes with raised heels[79], [80] and raised toes[80], [81] have been shown to increase whole body energy consumption. There is a growing body of literature that examines how these devices impact biomechanics across scale[20], [27], [34], [49], [73], [74], [78], [80], [82]–[84]. However, the mechanism linking altered biomechanics and whole-body metabolic cost remains unclear for human walking. Though exoskeletons are typically designed to reduce the biological joint moment, or work, these augmentations do not directly explain changes in energetic costs. Discrepancies in changes in the biological system and whole-body energetics help to highlight the need to directly investigate the mechanism of how changes in biomechanics impact energy expenditure. For example, a previous study found conditions with passive ankle exoskeleton assistance that led to reductions in center of mass work during hopping, but an increase in metabolic energy [74]. Locally, a previous study found conditions with reductions in ankle mechanical work during hopping with an elastic ankle exoskeleton, but an increase in metabolic energy [49]. Additionally, previous studies found passive conditions that achieved metabolic cost reductions, while requiring the biological ankle to do more mechanical work[19]. When considering joint power, a previous study found assistance conditions during walking in a passive ankle device that increased metabolic cost of walking, but reduced biological

36

ankle power [19]. Finally studies in both exoskeletons[19] and high heeled shoes[80], [85], [86] found conditions that reduced ankle moment, or muscle force generation, but counterintuitively led to increase metabolic costs during walking.

While joint work, powers, and moments can correlate to energetic cost reductions [24], the previously described discrepancies suggest that joint mechanics cannot fully explain changes in energetics. To investigate the link between altered biomechanics and change in whole body metabolic cost, it is important to look further into muscle-tendon dynamics. Specifically, the triceps-surae muscles because they contribute the majority of force necessary for vertical support and forward progression during walking[16], [17], [87]. Previous work in exoskeletons suggests a link between soleus muscle fascicle operating length and metabolic costs during walking[20]. Additionally, we previously showed that during isometric ankle plantarflexion, decreasing soleus fascicle operating length by 17%, increased metabolic cost by 208% [88]. Fascicle operating lengths may not solely explain metabolic costs. Although not directly measured, a previous study presumed that high heels shift muscles to shorter fascicle operating lengths, decreasing force-length (FL) potential, and presumed raised toe shoes increase fascicle lengths, increasing FL potential, but found metabolic increases in both shoe conditions [80]. Another study directly found shorter gastrocnemius fascicle lengths in high heeled walking, but their muscle activity results conflicted with other high heeled literature, noting a decrease in muscle activity[89]. Controlled studies that directly measure whole body energetics, muscle activity, and fascicle dynamics in multiple conditions can provide insight to the mechanistic link between altered biomechanics and locomotion performance.

An emerging neuro-mechanical principal suggests that active muscle volume, encompassing force demand, and muscle fascicle force-length and force-velocity

37

dynamics, is what drives energy expenditure [35]. A model proposed for AMV is as follows:

$$V_{act} = \frac{F_{act}*l_m}{\sigma*FL*FV} \tag{1}$$

Where F_{act} is the active muscle force, l_m is the length of the muscle, σ is the specific tension of the muscle, FL is the force-length influence and FV is the force velocity influence of the muscle. Decreases in force demand can be offset by either worse force-length (i.e. operating at shorter, less optimal lengths) or force-velocity (i.e. operating at faster, less optimal shortening velocities) potential. Or increases in force demand can be offset by either better force-length (i.e. operating at longer, more optimal lengths) or force-velocity (i.e. operating at slower, more optimal shortening velocities, or actively lengthening) potential.

The purpose of this study was to dive deeper into how shifting calf muscle dynamics impacts metabolic energy expenditure. We used modified footwear, to systematically incur more plantar-flexing and more dorsi-flexing via raised heels and raised toes, respectively. We hypothesized that walking in raised heels would decrease triceps-surae operating lengths and the raised toes would increase triceps-surae operating lengths. We hypothesized that whole body metabolic costs would be driven by the local calf muscle active muscle volume.

3.2 Methods

3.2.1 Participants

15 total volunteers completed the experimental protocol. None of the participants had self-reported musculoskeletal injuries at the time of collection. Participants were randomly split into two experimental groups; raised heels and raised toes. None of the participants were habitual high heel wearers. The raised heel group consisted of 8

participants, 3 women and 5 men, ages 28.4±2.5 years, heights 171.64±9.56 cm, and body mass 72.56±14.83 kg. The raised toe group consisted of 7 participants, 2 women and 5 men, ages 30.4±7.1 years, heights 173.69±10.59 cm, and body mass 75.36±18.17 kg. Every participant gave written informed consent prior to completing the protocol. The study protocol was approved by the Georgia Institute of Technology Central Institutional Review Board.

3.2.2 Modified Shoes

We fabricated raised heel and raised toe shoes for this experimental protocol under the guidance of a certified prosthetist/orthotist. We started with a commercial shoe that has a level outsole (Chuck Taylor All-Star Low Top, Converse, Boston, MA, USA). We modified the soles of the shoes with Ethylene-Vinyl Acetate (SoleTech Inc., Salem, MA, USA) and rubber tread (Vibram Corporation, North Brookfield, MA, UAS) to create high heel shoes with 14° plantar-flexion a high toe shoes with 8.5° dorsi-flexion. Participants also wore unmodified flat shoes that were mass matched to their modified via lead shot in a pouch secured to the top of their shoes.

3.2.3 Experimental Protocol

Each participant completed two experimental sessions: one metabolic and on biomechanics collection, which were randomized and performed within a week of each other. For metabolic collections, participants arrived at the laboratory in the morning following an overnight fast. Upon arrival, we measured participant height, mass, and Achilles tendon moment arm during standing. Next participants completed a 5-minute standing resting trial while breathing into a mouth- piece that channeled expired air to a metabolic cart (TrueOne 2400, ParvoMedic, Sandy, UT). Participants completed 8 randomized 5-minute walking trials on a split belt instrumented treadmill (Bertec

Corporation, Columbus, OH, USA) while breathing expired air into the metabolic cart: experimental and mass matched flat shoes at 0.5,0.9,1.3 and 1.7 m/s. For biomechanics collections, we shaved participant's leg hair and used electrode preparation gel to lightly abrade the skin superficial to their lateral soleus (SOL), lateral gastrocnemius (LG), tibialis anterior (TA), vastus medialis (VM), rectus femoris (RF), biceps femoris (BF), gluteus medius (GMED) and gluteus maximus (GMAX) (NuPrep, Weaver and Co., Aurora, CO). Next, we placed bipolar surface electrodes over the skin superficial to each respective muscle belly and in approximately the same orientation as the muscle fascicles (Delsys Inc., Natick, MA). We secured a linear-array B-mode ultrasound probe to the skin superficial of each participant's right medial gastrocnemius and soleus (Telemed, Vilnius, Lithuania). Next, we isolated each of the tested 8 leg muscles (SOL, LG, TA, VM, RF, BF, GMED, and GMAX) and participants performed maximum voluntary contractions. We then placed we placed reflective markers on the left and right side of each participant's lower body and upper body (superficial to the head of the 1st and 5th metatarsal, posterior calcaneus, medial and lateral malleoli, lateral mid-shank, medial and lateral knee-joint center, lateral mid-thigh, greater trochanter, anterior superior iliac crest, posterior superior iliac crest, sacrum, T10 thoracic vertebrae, C7 cervical spine, shoulders, xiphoid process, right scapula and sternum). We captured motion capture data during the collection using a 3D reflective marker motion capture system (Vicon Motion Systems, UK). Participants walked two minutes at each speed in experimental and mass matched flat shoes at 0.5, 0.9,1.3 and 1.7 m/s. Walking trials were randomized. We recorded vertical and anterior–posterior ground reaction forces (GRFs) (1000 Hz) as well as motion capture (200 Hz) data and ultrasound (100Hz) data during the last 30 seconds of each trial.

3.2.4 Metabolic Cost Measurements

During the standing resting trial and each walking trial, we used open-circuit expired gas analysis to record the participant's rates of oxygen uptake ($\dot{V}o2$) and carbon dioxide production ($\dot{V}co2$). During each trial we monitored participant's respiratory exchange ratio (RER) to see that they primarily relied on aerobic metabolism during walking; indicated by an RER ≤ 1 [90]. We removed 8 metabolic values out of 120 from our analysis because the participants RER was >1, indicative of fat and/or carbohydrate oxidation[90]. We averaged breath by breath data over the last 2-min of each trial and used a standard equation[90] to calculate steady state metabolic power (W). To obtain mass-normalized net metabolic power (W/kg) we subtracted the participant's resting metabolic power from each walking trial and divided by participant mass. Finally, we divided by walking speed (0.5-1.7m/s) of each trial to get a net cost of transport curve (J/kg).

3.2.5 Muscle Fascicle Dynamics

To determine soleus and lateral gastrocnemius fascicle dynamics, we recorded B-mode ultrasound images containing the posterior-lateral soleus compartment, and lateral gastrocnemius compartment in the same frame, using a linear probe ultrasound system. We recorded soleus fascicle images during the last 15 seconds each 2-minute walking trials. Within this trial, we postprocessed soleus and gastrocnemius fascicle lengths and pennation angles throughout five consecutive moment generation cycles using a semiautomated tracking software[91]. We filtered soleus fascicle pennation angle and length using a fourth-order low-pass Butterworth filter (6 Hz) and then averaged the five cycles for each participant together. We took the derivative of each fascicle length cycle with respect to time to determine fascicle velocity. Due to image quality, we were unable to collect 14 fascicle trials out of 60.

3.2.6 Joint Kinematics and Kinetics and Muscle-Tendon Force

We filtered marker positions at 6 Hz. We calculated joint angles from the 3D marker set data using OpenSim. Joint velocity was calculated as the first derivative of joint angle. We performed inverse dynamic analysis using marker data and measured GRFs to calculate net joint moments (Nm/kg), using Opensim. We calculated joint power as a product of the joint velocity and joint moment. We estimated force on the triceps-surae by dividing the ankle moment by the measured Achilles tendon moment arm for each participant during standing. We calculated the force on the SOL and LG by taking the whole muscle tendon force, scaling it by estimated PCSA[92] and dividing by cosine of measure pennation angle. For each participant, we calculated and average of 5 strides for each walking conditions by time normalizing each stride between heel-strikes to obtain a single normalized stride per participant, per condition.

3.2.7 Cumulative muscle activity

We band-pass filtered raw SOL, LG, TA, VM, RF, BF, GMED and GMAX signals between 40 and 200 Hz, full wave rectified the filtered signals, smoothed the filtered signals with a 50 ms moving window and normalized each trial to each muscles processed peak MVC. To calculated cumulative muscle activity, we took the average of 5 strides per muscle per condition per participant, and integrated with respect to cycle time, then divided by cycle time to get the normalized cycle averaged cumulative muscle activity. Weighted averages of whole leg metabolic were taken by summing each of the 8 muscle's average activity and multiplying by relative PCSA from a previous study[92]. Due to technical issues, we were unable to collect 2 participant's EMG data out of 15.

3.2.8 Active Muscle Volume (AMV) Modeling

A previous study suggests that metabolic energy expenditure is well-explained by active muscle volume (V_{act}) which can be modeled by the following equation[35]:

$$V_{act} = \frac{F_{act} * l_m}{\sigma * FL * FV}$$

Where F_{act} is the active muscle force, l_m is the length of the muscle, σ is the specific

tension of the muscle, FL is the force-length influence and FV is the force velocity

influence of the muscle. We modeled V_{act} using this equation for the SOL and LG,

assuming no passive muscle contribution of the calculated forces on each muscle. We

used previous relationships for operating length of each muscle relative to l_0[93], to

calculate l_0 from our tracked ultrasound trials for each muscle. We used a previously

published value for specific tension of the muscle, 20 (N/cm^3)[94]. We calculated V_{max} as

using and approximation of $4.4l_0s^{-1}$ for type I fibers and $16.7\ l_0s^{-1}$ for type II fibers[30],

and assumed a composition of 81% type I and 19% type II for SOL and 50% type I and

50% type II for LG[95]. We normalized measured fascicle force and velocities by our

calculated l_0 and V_{max} then used previously published normalized FL[96] and FV[97]

curves to calculated their contributions to active muscle volume. We averaged 5 strides

per condition at 1.3 m/s for each participant, then integrated with respect to cycle time

and divided by cycle time to calculate an average AMV per participant per condition.

Along with AMV, we assessed force economy of the soleus and gastrocnemius as force

per unit activation (F/act), which should be proportionate to the force potential (FL*FV).

3.2.9 Statistics

Unless otherwise specified, we performed all statistical tests within the raised toe and

raised heel groups independently. We performed linear mixed models to determine the

influence of shoe (flats vs toes or flats vs heels) on net metabolic power, peak calf MTU

force, soleus and medial gastrocnemius fascicle length at peak force, and cumulative

EMG of the soleus, medial gastrocnemius, and a weighted sum of all the measured leg

muscles. We set the significance level (a =0.05) and performed statistical analyses using RSTUDIO software (RSTUDIO, Inc., Boston, MA).

3.3 Results

Metabolic cost of transport increased from flat to experimental shoes in both the raised toe and raised heel group (Fig. 1)
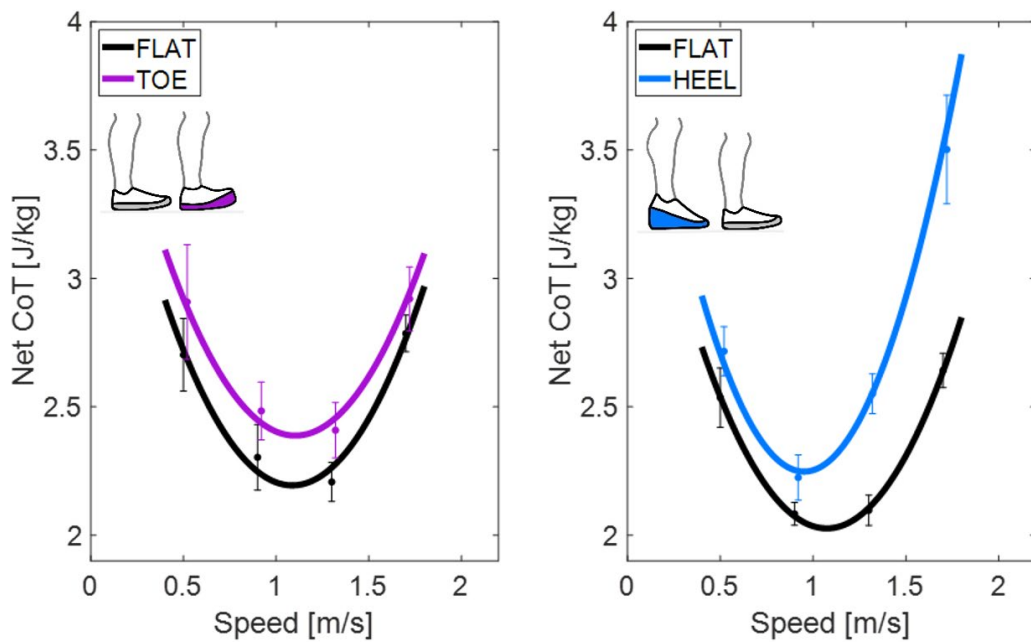
Figure 1. Net cost of transport curves for flats (black) vs toes (purple) and flats (black) vs heels (blue) at 0.5 m/s, 0.9 m/s, 1.3 m/s and 1.7 m/s/

The raised to group has increased dorsiflexion throughout the entire gait cycle compared to flat shoes (Fig. 2A). Conversely, the raised heel group had increased plantar flexion compared to flat shoes except at push off where the ankle angles are matched (Fig. 2A).

Ankle moment increased in the raised toe group compared to mass-matched flat shoes

and decreased in the raised heel group (Fig. 2B).

Figure 2. A) Ankle angle [degrees] during walking at 1.3 m/s in flats(black) vs toes (purple) and flats (black) vs heels (blue). B) Ankle moment [Nm/kg] during walking at 1.3 m/s in flats(black) vs toes (purple) and flats (black) vs heels (blue).

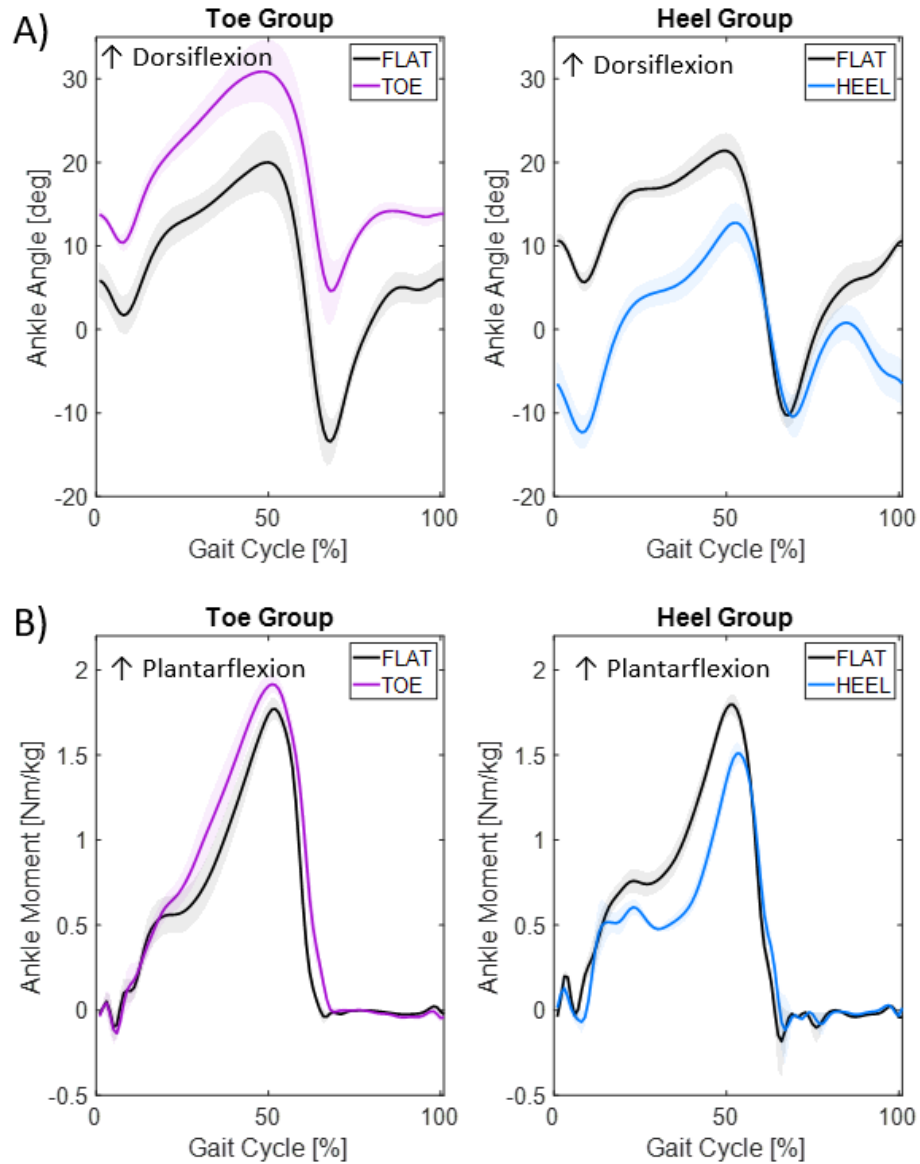The raised toe group increased peak force on the triceps-surae muscle tendon unit (MTU) by 8% (p<0.001) (Fig.3). With all other biomechanical factors constant, increased force demand would raise metabolic costs in raised toes vs flats. Conversely, the raised heel group decreased peak force on the triceps-surae MTU by 16% (p<0.001) (Fig.3). With all other biomechanical factors constant, decreased force demand would raise metabolic costs in raised heels vs flats.

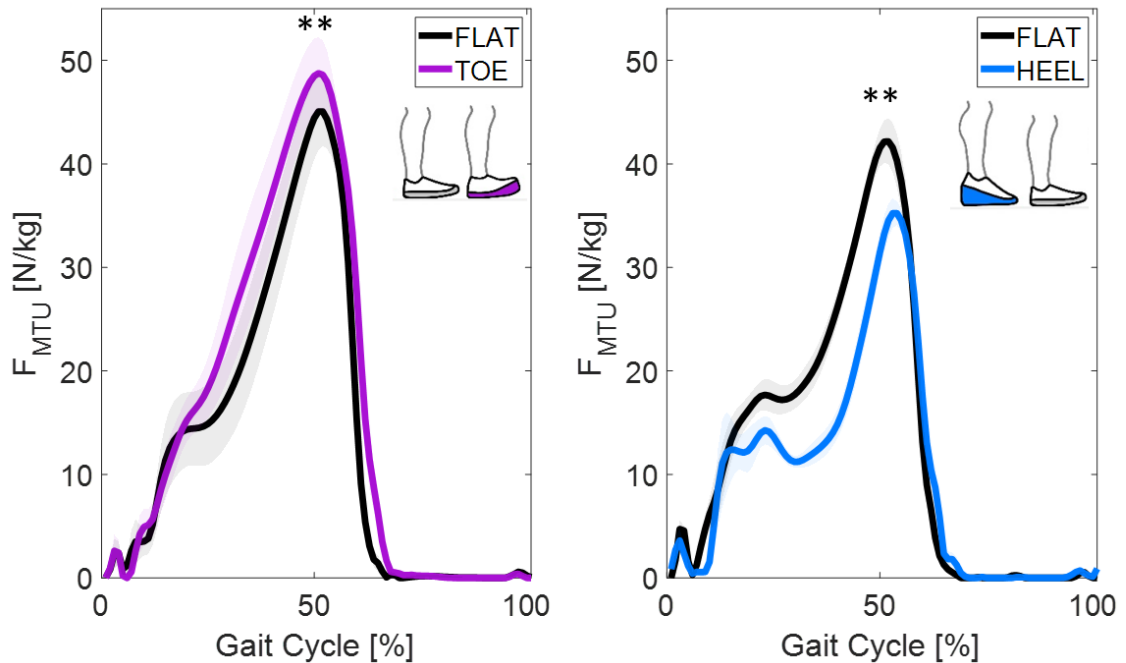**Figure 3.** Triceps-surae muscle tendon force timeseries for flats (black) vs toes (purple) and flats (black) vs heels (blue). **Indicates p<0.001 peak force.

The raise toes increased soleus (SOL) and medial gastrocnemius (GAS) fascicle operating lengths throughout the gait cycle, while raised heels decreased the fascicle operating lengths of both muscles throughout the gait cycle (Fig. 4A). The experimental

shoes changed fascicle velocities for both the heel and toe groups (Fig. 4B). In raised toes, length of SOL and GAS fascicles at peak force increased by 10.6% (p=0.082) and 7.6% (p=0.028) respectively (Fig. 4C). In raised heels, length of SOL and GAS fascicles at peak force decreased by 18.9% (p<0.001) and 13.4% (p<0.001) respectively (Fig. 4C). With all other biomechanical factors constant, increased FL potential via longer fascicle operating lengths would decrease metabolic costs in raised toes compared to mass-matched flat shoes. Conversely, with all other biomechanical factors constant, decreased FL potential via shorter fascicle operating lengths would increase metabolic costs in raised heels compared to mass-matched flat shoes.
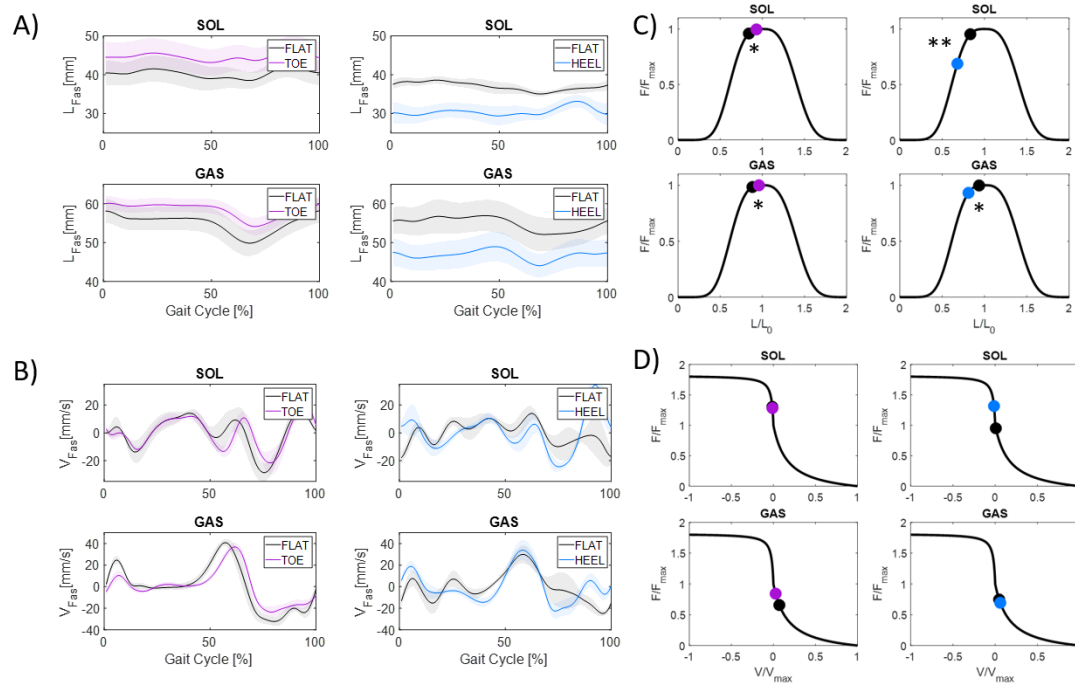
Figure 4. A) Soleus (SOL) and medial gastrocnemius (GAS) fascicle operating length for walking at 1.3 m/s B) SOL and GAS fascicle operating velocity for walking at 1.3 m/s C) Mapped SOL and GAS lengths at peak force on a normalized FL curve. **Indicates p<0.001, *Indicates P<0.05 D) Mapped SOL and GAS fascicle velocities at peak force on a normalized FV curve.

47

We modeled active muscle volume (AMV) using a previously established theory (Eq. 1). Time series graphs (Fig. 5A) of AMV over the gait cycle in raised toes vs flats for SOL and GAS as well as average AMV over the gait cycle (Fig. 5C) did not show a significant difference. In raised heels vs flats (Fig. 5B, and Fig. 5C) the soleus did not have a significant difference in modeled AMV, while GAS AMV significantly decreased in high heels vs mass matched flats (Fig. 5C)
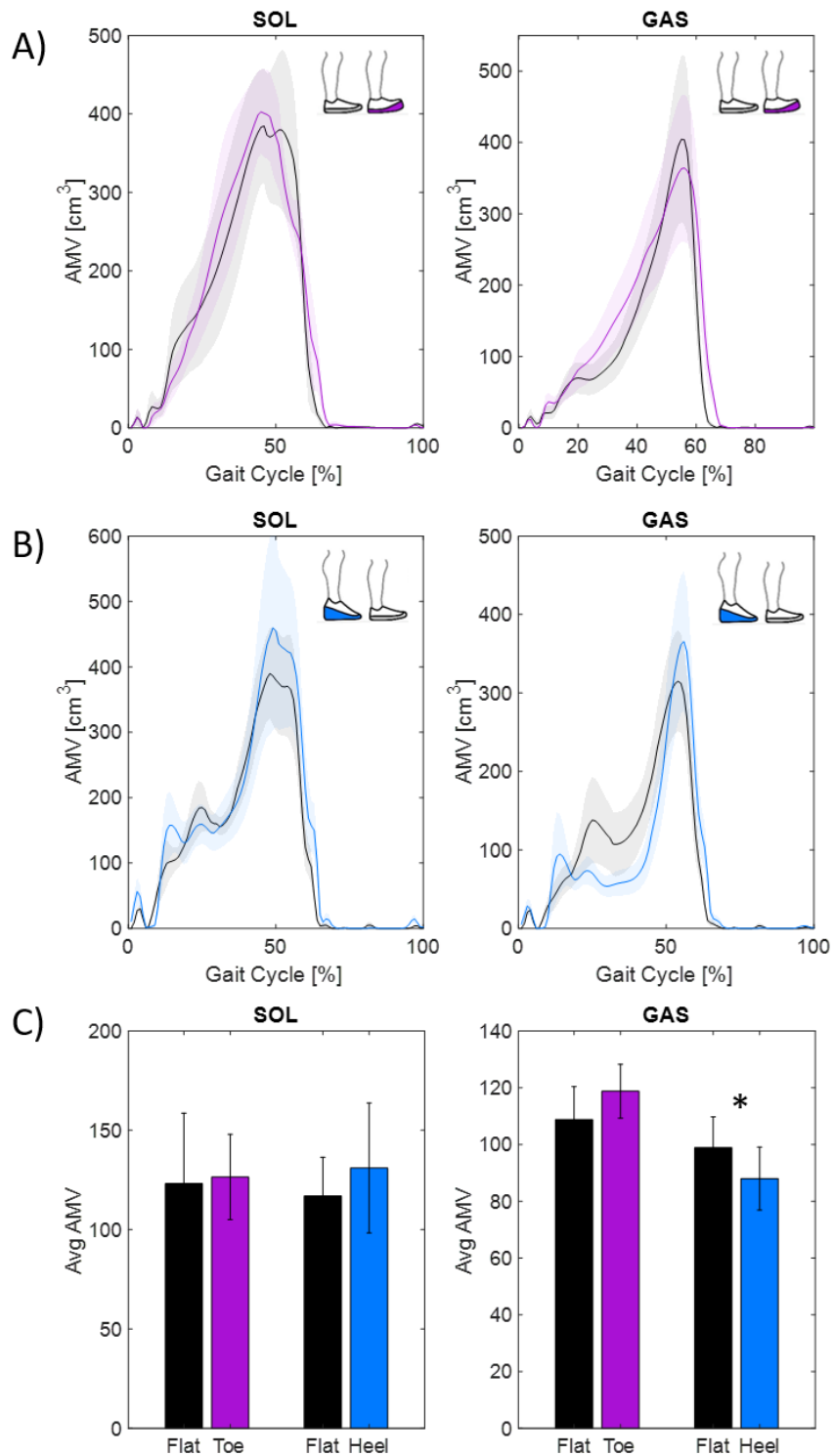
Figure 5. A) Time series AMV for SOL and GAS in flats (black) and toes (purple) B) Time series AMV for SOL and GAS in flats (black) and heels (blue) C) Average SOL and GAS AMV for flats vs toes and flats vs heels. *Indicates P<0.05

Cumulative EMG for SOL was not significantly different in raised toes vs mass-matched

flat shoes (Fig. 6C). However, cumulative EMG for GAS significantly increased by 4.6%

(p=0.004) (Fig. 6C), and a weighted average of all the leg muscles measured (SOL, LG,

TA, VM, BF, RF, GMED, and GMAX) significantly increased by 20% in raised toes vs

mass-matched flat shoes (Fig. 6D). In the raised heels, cumulative EMG for SOL

significantly increased by 43% (p=0.001) (Fig. 6C), for GAS significantly increased by

43% (p=0.036) (Fig. 6C), and for all the measured leg muscles increased by 28.8%

(p=0.015) vs mass matched flat shoes (Fig. 6D).
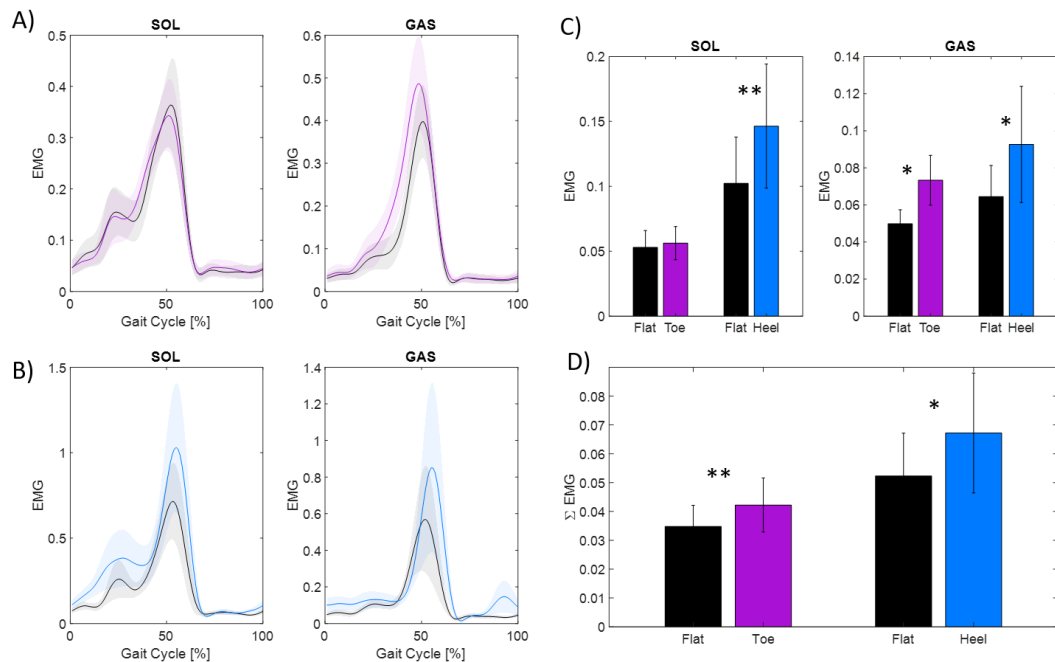
Figure 6. A) Time series EMG for SOL and GAS in flats (black) and toes (purple) B)Time series EMG for SOL and GAS in flats (black) and heels (blue) C) Cumulative SOL and GAS EMG for flats vs toes and flats vs heels. **Indicates p<0.001, *Indicates P<0.05 D) Weighted sum of cumulative EMG for all measured leg muscles (SOL, LG, TA, VM, BF, RF, GMED, and GMAX) for flats vs toes and flats vs heels. **Indicates p<0.001, *Indicates P<0.05

Force economy (force/activation) did not change in raised toes, due to the tradeoff of increased force demand (increased muscle-tendon unit force) and increased force potential (shift to longer operating lengths). On the other hand, high heels decreased force demand (decreased muscle-tendon unit force) and increased force potential (shifts to shorter operating lengths). Force economy of both the soleus and medial gastrocnemius decreased in the heel group (Fig. 7).
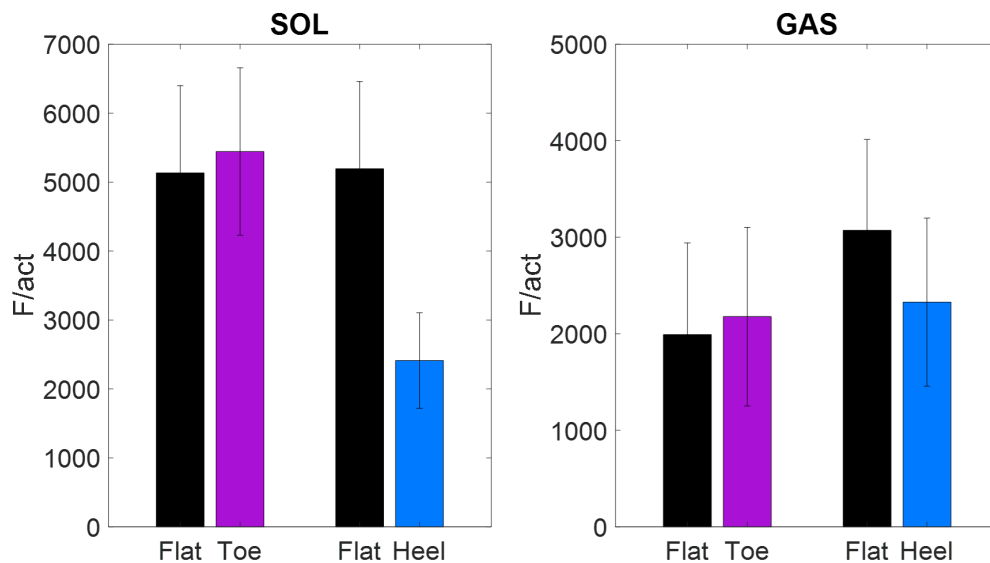
Figure 7. Average force economy, force per activation of the soleus and gastrocnemius muscles in flats vs toes and flats vs heels

3.4 Discussion

The purpose of this study was to investigate how changing biomechanics of the triceps-surae muscle impacts whole-body metabolic energy expenditure. We tested one group in raised toes, that increased ankle dorsi-flexion at the ankle vs mass-matched flat shoes and the other in raised heels, that increased ankle plantar flexion vs mass-matched flat

shoes. We measured whole body metabolic costs and biomechanical outcomes from joint down to the muscle fascicle level.

We found that both raised toes and raised heels increased metabolic cost across tested speeds (0.5, 0.9, 1.3, and 1.7 m/s) compared to mass-matched flat shoes. The tradeoff of biomechanical impacts on metabolic costs can be seen in both experimental shoes impact on the triceps-surae muscle-tendon unit (MTU) force, fascicle lengths and fascicle velocities. The raised toes significantly increased peak ankle moment and MTU force but increased force-length potential via significantly long soleus and medial gastrocnemius operating lengths. Conversely, the raise heels significantly decreased peak ankle moment and MTU force but decreased force-length potential via significantly shorter soleus and medial gastrocnemius operating lengths. Contrary to our hypothesis, modeled active muscle volume (AMV) was not significantly different in soleus for either experimental shoe and AMV of the gastrocnemius muscle was unchanged for raised toes but significantly decreased raised heels. However, both experimental shoes increased EMG activity in the calf muscles as well as the weighted whole leg cumulative activity.

Our metabolic and muscle activity levels are consistent with previous studies in raised toes [80], [81] and raised heels [79], [80]. Our fascicle lengths in high heels are consistent with a previous study[89], though they reported EMG activity decreased with high heels, contrary to our results and other literature.

Due to trade-offs in force, and force length and force velocity potential and AMV results that do not trend with whole body metabolic costs, our results have a lack of resolution for determining if local changes at the calf muscle drive whole body metabolic costs. When considering EMG, our local calf changes do trend with whole body metabolic

52

costs, but so does the cumulative leg muscles. Further investigation into knee and hip joints can provide insight into potential proximal compensation.

In the toe group kinematics, there does not appear to be any compensations for the increased dorsiflexion angle at the knee or the hip (Supplemental Fig. 1). While the heel group has increased knee flexion in early stance and decreased knee flexion in late stance and swing (Supplemental Fig. 1). Both raised toes and raised heels yielded significant decreases in ankle power at push-off (Supplemental Fig. 2). Previous work highlights that populations with decreased ankle push-off power, for example aging, people with amputation, or stroke, compensate with increased hip power [98]–[103]. Interestingly, neither raised heels nor raised toes appear to have compensation at the hip in power or moment. The raised heels have increased knee power in late stance and decreased power at push off. Compensation in the raised heels can also be seen in the increased vastus medialis cumulative activity, a knee extensor.

While local EMG at the plantar flexors correlated with metabolic costs, our model for active muscle volume (Eq. 1), did not predict participant's metabolic energy expenditure or muscle activity. We expected modeled AMV to correlate both with metabolic cost and EMG, but our results show that it did not for either.

Active muscle volume can be broken down into a ration between force demand and force potential. Previous studies have explored force potential and related it to metabolic energy costs [30], [104]–[106]. In line with those studies, examination of the muscle dynamics in our experiment also reveals changes in the muscle force potential that are likely related to the activation required to produce force (Fig. 4) While muscle dynamics indicate the economy of contraction is changing, the amount of force demand also changed because walking in the experimental shoes vs flats, the level of force required to move was not fixed (Fig. 3). So, that creates a potential discrepancy between the

53

EMG results and the AMV results. Our AMV model that incorporates Hill-type muscle models may not capture the relative weight of force demand, muscle operating length, and muscle operating velocity on whole body metabolic cost.

In a previous study we also showed discrepancies between our AMV model and energetic costs, in isolated ankle contractions where the force of the task was fixed [88]. This could also be due to the weightings in our model, or it could be that something is missing from the model. Other studies suggest models for metabolic cost that suggest different ways heat can be liberated during contractions that we do not account for in our model [107], [108].

In our AMV model (Eg. 1) we are borrowing a model of muscle force production (FL and FV) and trying to directly relate it to metabolic energy costs. The discrepancies in our AMV results and metabolic results could be because the factors from the force production that contribute to metabolic energy expenditure should not be weighted in the same ways, as our model suggest. Or, there could be missing factors in our model that contribute to metabolic costs such as enthalpy costs, force-length-activation dependency, or history dependent muscle phenomena that enhance or depress force. More experiments on isolated muscle and isolated joints can help uncover the mechanism for metabolic energy expenditure. Specifically, experiments that can independently manipulate what we believe are the primary factors that are important for energetics costs.

3.5 Supplemental Figures
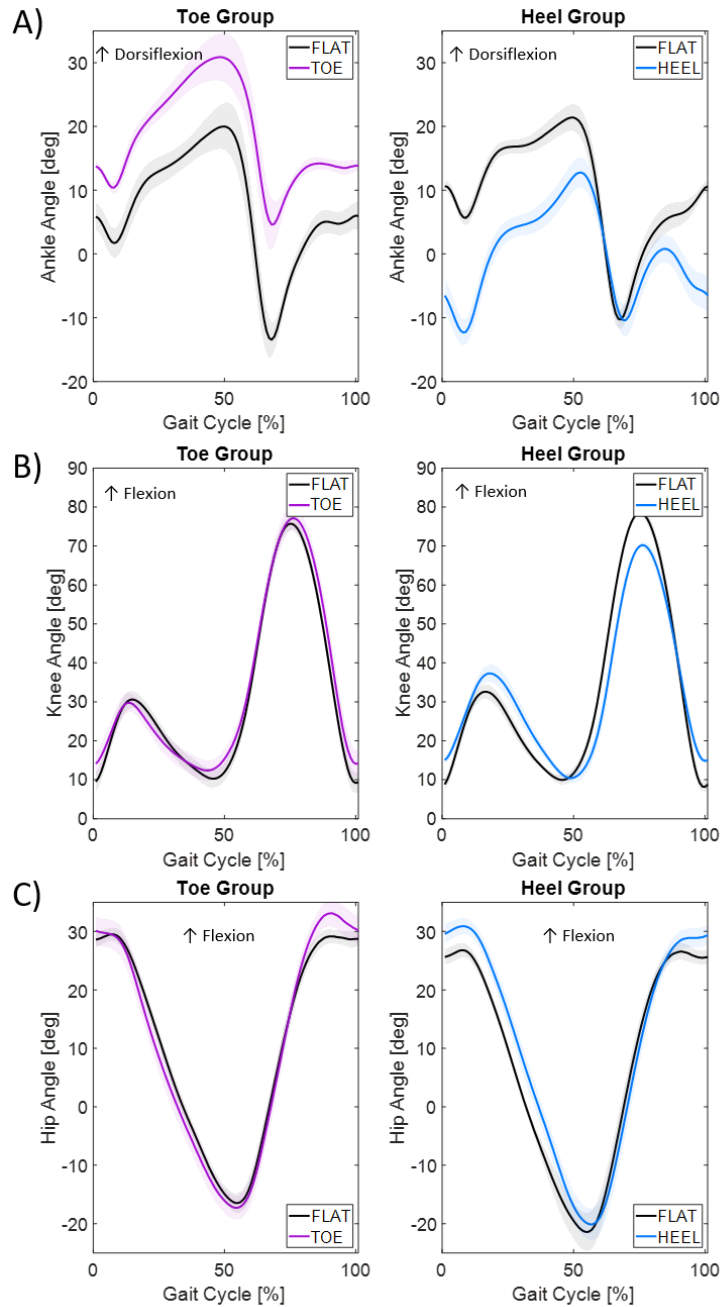
Supplemental Figure 1: A) Time series ankle angle for flats (black) vs toes (purple) and flats (black) vs heels (blue) B) Time series knee angle for flats (black) vs toes (purple) and flats (black) vs heels (blue) C) Time series hip angle for flats (black) vs toes (purple) and flats (black) vs heels (blue)
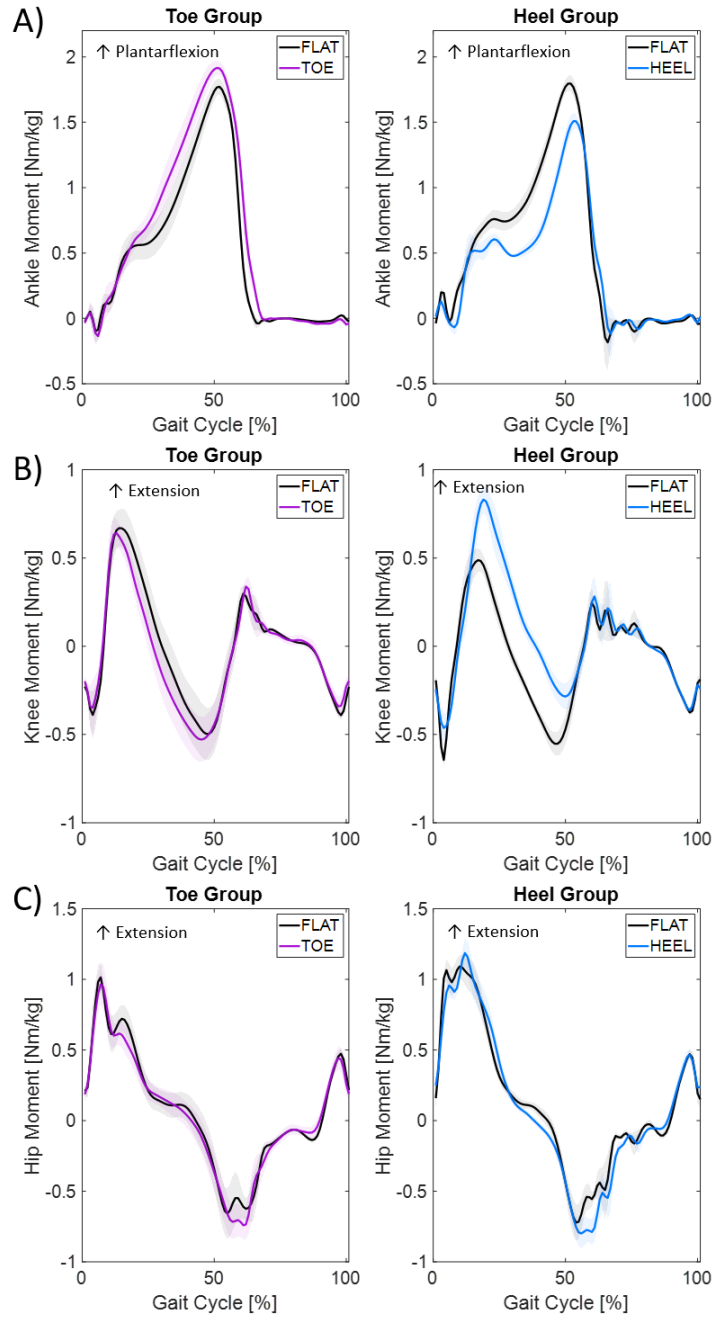
Supplemental Figure 2: A) Time series ankle moment for flats (black) vs toes (purple) and flats (black) vs heels (blue) B) Time series knee moment for flats (black) vs toes (purple) and flats (black) vs heels (blue) C) Time series hip moment for flats (black) vs toes (purple) and flats (black) vs heels (blue)
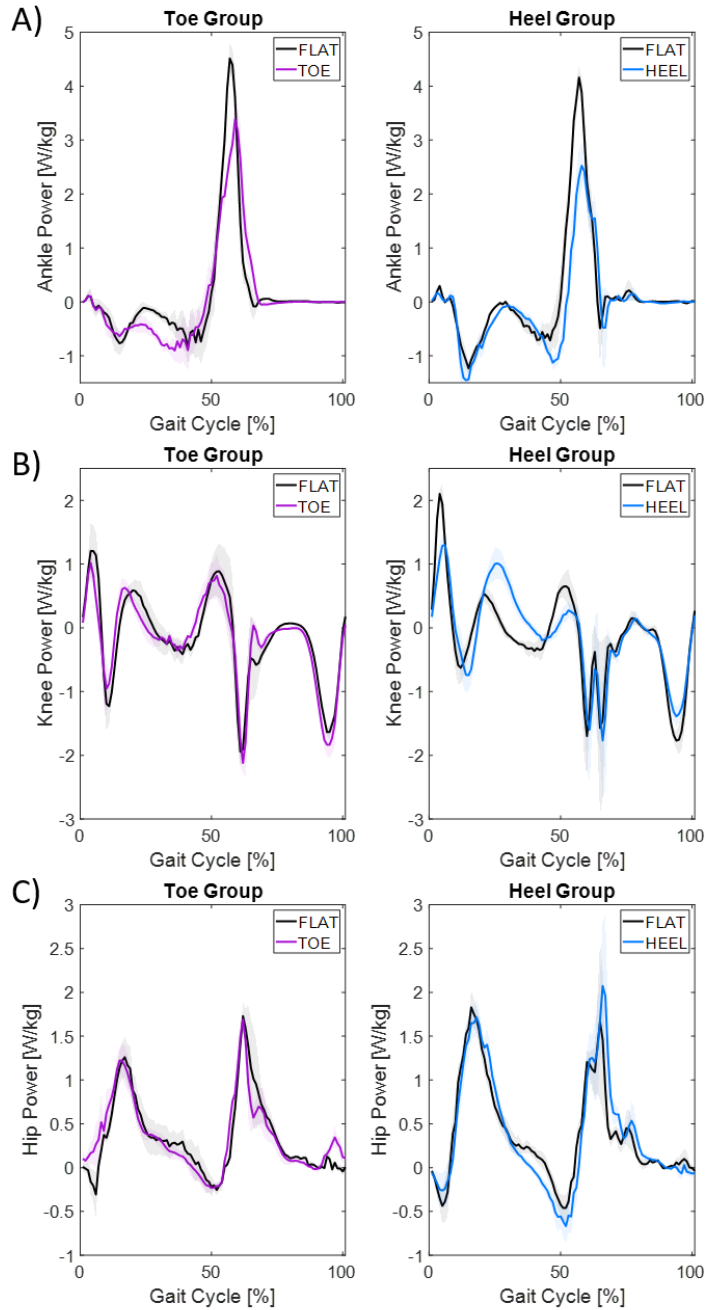
Supplemental Figure 3: A) Time series ankle power for flats (black) vs toes (purple) and flats (black) vs heels (blue) B) Time series knee power for flats (black) vs toes (purple) and flats (black) vs heels (blue) C) Time series hip power for flats (black) vs toes (purple) and flats (black) vs heels (blue)

57
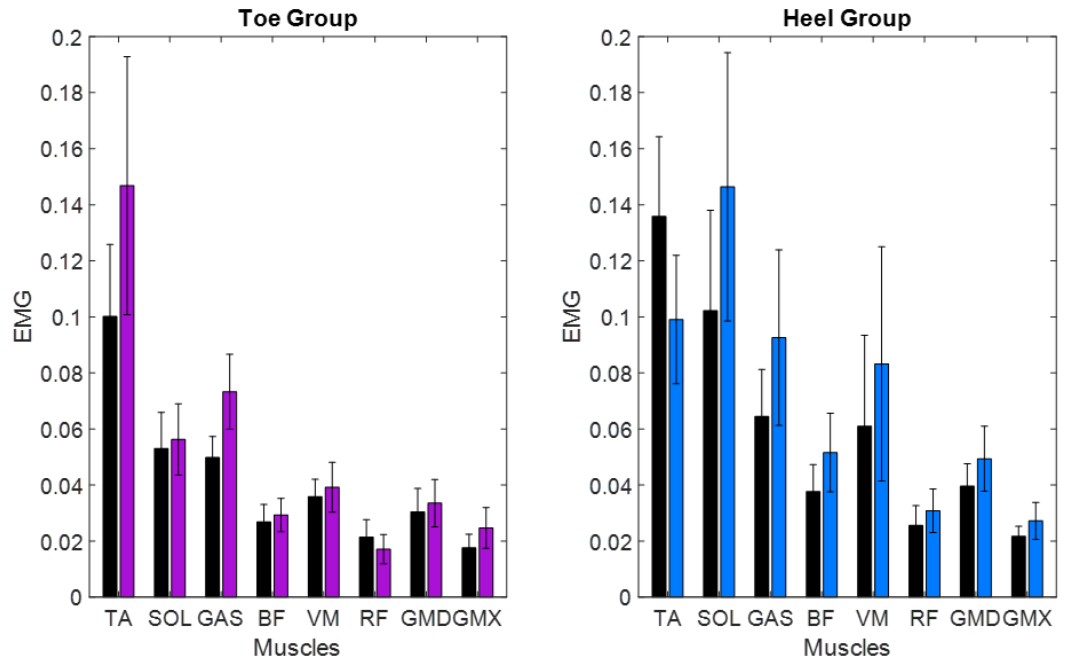
Supplemental Figure 4: Cumulative EMG for each of the 8 tested leg muscles in flats (black) vs toes (purple) and flats (black) vs heels (blue)

CHAPTER 4

Relatively Small Changes in Foot-Ankle Mechanics Over Months Alters Muscle-Tendon Structure

4.1 Introduction

Form follows function. A growing body of literature demonstrates that both skeletal muscle and tendon adapts to their mechanical environments. Skeletal muscle architecture is designed to meet functional demands[109]. Previous work suggests that if a muscle is forced to operate in an overstretched positions, longitudinal fascicle growth occurs [110]. Under lengthening conditions, skeletal muscle fascicles lengths increase by adding sarcomeres in series[111]. Fascicles that are trained at shorter muscle-tendon unit lengths have been shown to remodel to be absolutely shorter[111]. Additionally, computational modeling of chronic muscle shortening suggests that muscle adapts to a new functional length by chronic loss of sarcomeres in series[112]. Following concentric or eccentric exercise, skeletal muscles hypertrophy[4]. On the other hand, muscle atrophy has been observed in chronic unloading and disuse studies[36], [37]. Tendons also adapt to their mechanical environments[113]. They are sensitive to several factors including strain magnitude, cycle duration, cycle frequency and intervention duration [45], [47], [48]. Exercise studies have reported increased stiffness, modulus of elasticity, and cross-sectional area[43]–[45]. Alternatively, tendon atrophy has been observed following chronic unloading and disuse studies[7], [46], [114].

Most muscle and tendon adaptation knowledge comes from exercise intervention studies that include low cycle numbers and large strains. Literature suggests tendon is not likely to hypertrophy unless interventions are above ~4.5-6.5% strain[115]. However, cross

sectional studies of habitual high heel wearers report sizable increases in Achilles tendon size and stiffness and shortening of the gastrocnemius muscle fascicles, compared to people who do not wear high heels [82], [84], [116]. These studies suggest chronic adaptation in both muscle and tendon structure related to long term high heel use[84]. This indicates that even with small changes in musculoskeletal loading (i.e. low strain), muscle-tendon remodeling may occur over long time scales if the number of cycles is plentiful.

The purpose of this study was to determine how relatively small changes in foot ankle mechanics remodels the underlying MT structure following relatively large number locomotion cycles. We altered foot ankle mechanics in daily activities over a 14-week intervention via modified footwear and measured leg MT structural properties pre and post intervention. We hypothesized that footwear that increased/decreased muscle operating lengths during daily use would lead to muscles that were relatively longer/shorter after intervention. We also hypothesized that devices that decreased/increased force on the calf MT over a large number of cycles would lead to tendons that were less/more stiff after intervention.

4.2 Methods

4.2.1 Participants

17 total volunteers completed the experimental protocol. None of the participants had self-reported musculoskeletal injuries at the time of collection. Participants were randomly split into two experimental groups; raised heels and raised toes. None of the participants were habitual high heel wearers. The raised heel group consisted of 8 participants, 3 women and 5 men, ages 28.4±2.5 years, heights 171.64±9.56 cm, and body mass 72.56±14.83 kg. The raised toe group consisted of 6 participants, 2 women

and 4 men, ages 30.4±7.1 years, heights 173.69±10.59 cm, and body mass

75.36±18.17 kg. Every participant gave written informed consent prior to completing the

protocol. The study protocol was approved by the Georgia Institute of Technology

Central Institutional Review Board.

4.2.2 Modified Shoes

We fabricated raised heel and raised toe shoes for this experimental protocol under the

guidance of a certified prosthetist/orthotist. We started with a commercial shoe that has

a level outsole (Chuck Taylor All-Star Low Top, Converse, Boston, MA, USA). We

modified the soles of the shoes with Ethylene-Vinyl Acetate (SoleTech Inc., Salem, MA,

USA) and rubber tread (Vibram Corporation, North Brookfield, MA, UAS) to create high

heel shoes with 14° plantar-flexion a high toe shoes with 8.5° dorsi-flexion. Participants

also wore unmodified flat shoes that were mass matched to their modified via lead shot

in a pouch secured to the top of their shoes.

4.2.3 Protocol

After consenting to the study, participants wore flat shoes, that were mass matched to

their randomly assigned experimental shoes (raised heels or toes), during daily activities

for two weeks prior to the intervention. Participants then wore their experimental shoes,

and an activity tracker during daily activities for 14 weeks. Every week, participants self-

reported total daily steps, and daily steps in their experimental shoes. Participants came

into the laboratory at three timepoints for data collection: before the intervention (0

weeks), in the middle of the intervention (7-8 weeks), and at the conclusion intervention

(~14 weeks). There were two experimental days at each time point, a metabolics day

and a structural measurement day. For metabolic collections, participants arrived at the

laboratory in the morning following an overnight fast. Upon arrival, we measured

61

participant height, mass, and Achilles tendon moment arm during standing. Next

participants completed a 5-minute standing resting trial while breathing into a mouth-

piece that channeled expired air to a metabolic cart (TrueOne 2400, ParvoMedic, Sandy,

UT). Participants completed 8 randomized 5-minute walking trials on a split belt

instrumented treadmill (Bertec Corporation, Columbus, OH, USA) while breathing

expired air into the metabolic cart: experimental and mass matched flat shoes at

0.5,0.9,1.3 and 1.7 m/s. For the structural measurement day participants were

instrumented with a linear-array B-mode ultrasound probe to the skin superficial to the

junction of the right medial gastrocnemius (MG) and the Achilles tendon (Telemed,

Vilnius, Lithuania). They completed a series of isometric contractions on a dynamometer

(Biodex Medical Systems Inc., NY). At the end of the session, we measured Achilles

tendon cross sectional area using a B-mode ultrasound probe.

4.2.4 Achilles Tendon Stiffness and Cross-Sectional Area Measurements

We aligned Participants ankles with the dynamometer's axis of rotation, with their knee

fully extended and ankle at 90 degrees. Next, we secured their foot to a custom-built

pedal via ratcheting straps and padding, that was demonstrated to prevent ankle angle

changes >5° in piloting. Participants completed two isometric plantarflexion trials where

they were instructed to ramp up to maximum voluntary contractions. During the trials, we

captured the displacement of the Achilles tendon (AT)-MG junction via ultrasound, and

measured torque via the dynamometer. In post processing, we calculated ankle torque

during the trial by subtracting torque contributions from the dynamometer pedal and the

weight of the participants foot, approximated by body mass[96]. We approximated force

on the AT during the trial by dividing the ankle moment by the manually measured AT

moment arm. We measured the insertion of the AT into the calcaneus bone to the

bottom of the ultrasound probe. We manually tracked AT-MG junction location in the

ultrasound image at discrete time points, 0-100% of the maximum force achieved in 10% increments using ImageJ. AT stiffness was calculated as the slope of the force length curve between 50 and 100% of the maximum tendon force by means of linear regressions [69]. We excluded 2 out of 6 tendon stiffness measurements for the toe group, because we did not capture those participant's junction in the ultrasound frame when they went from standing to seated on the pre-intervention collections. We measured the AT cross section at 10% up the length of the free tendon using B-mode ultrasound during standing. We manually measured the cross-sectional area via ImageJ.

4.2.5 Metabolics Cost Measurements

During the standing resting trial and each walking trial, we used open-circuit expired gas analysis to record the participant's rates of oxygen uptake ($\dot{V}o2$) and carbon dioxide production ($\dot{V}co2$). During each trial we monitored participant's respiratory exchange ratio (RER) to see that they primarily relied on aerobic metabolism during walking; indicated by an RER ≤ 1 [90]. We removed 8 metabolic values out of 120 from our analysis because the participants RER was >1, indicative of fat and/or carbohydrate oxidation[90]. We averaged breath by breath data over the last 2-min of each trial and used a standard equation[90] to calculate steady state metabolic power (W). To obtain mass-normalized net metabolic power (W/kg) we subtracted the participant's resting metabolic power from each walking trial and divided by participant mass. Finally, we divided by walking speed (0.5-1.7m/s) of each trial to get a net cost of transport curve (J/kg).

4.2.6 Statistics

Unless otherwise specified, we performed all statistical tests within the raised toe and raised heel groups independently. We performed linear mixed models to determine the

63

influence of shoe (flats vs toes or flats vs heels) on net metabolic power, peak calf MTU force, soleus and medial gastrocnemius fascicle length at peak force, tendon stiffness, and muscle cross sectional area. We set the significance level (a =0.05) and performed statistical analyses using RSTUDIO software (RSTUDIO, Inc., Boston, MA).

4.3 Results

During walking in daily life, our intervention increased fascicle operating length in the high toes and decreased fascicle operating length in the high heels (Fig. 1). Peak muscle tendon (MT) force increased in high toes by 8% and decreased in high heels by 16% (Fig. 2.).
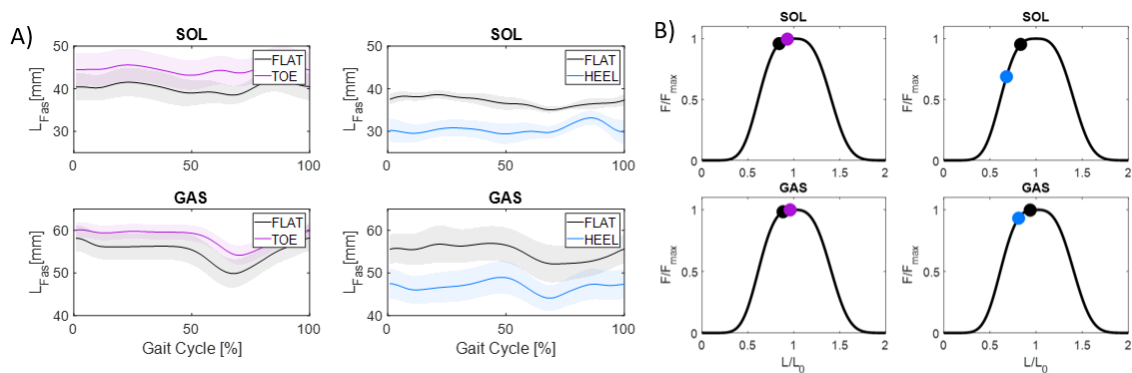
Figure 1. A) Soleus (SOL) and medial gastrocnemius (GAS) fascicle operating length for walking at 1.3 m/s B) Mapped SOL and GAS lengths at peak force on a normalized FL curve. **Indicates p<0.001, *Indicates P<0.05
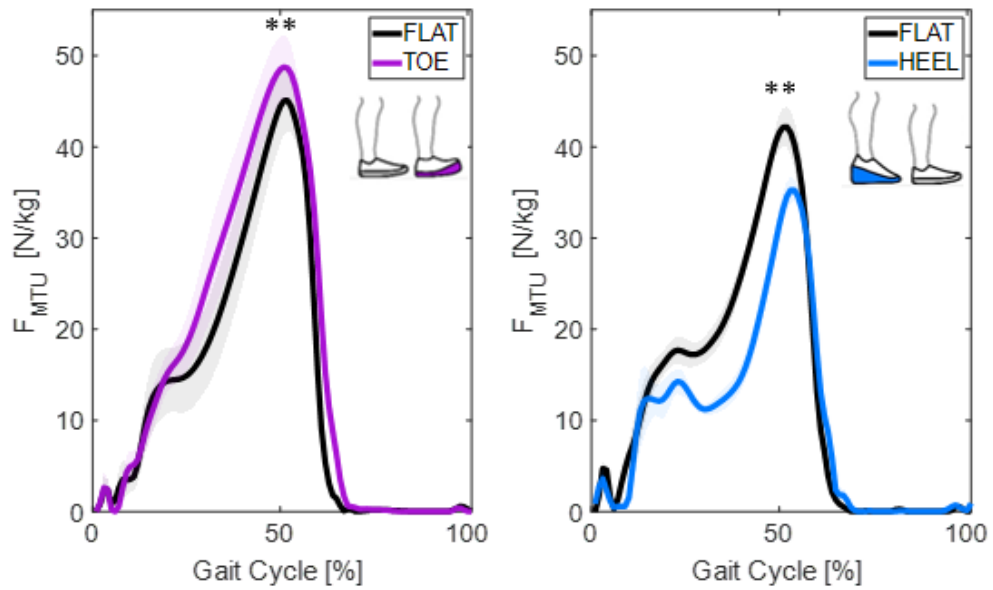
Figure 2. Triceps-surae muscle tendon force timeseries for flats (black) vs toes (purple) and flats (black) vs heels (blue). **Indicates p<0.001 peak force.

Overall, tendon stiffness did not change in either the high toes (p=0.456) or the high heels (p=0.449) groups (Fig. 3).
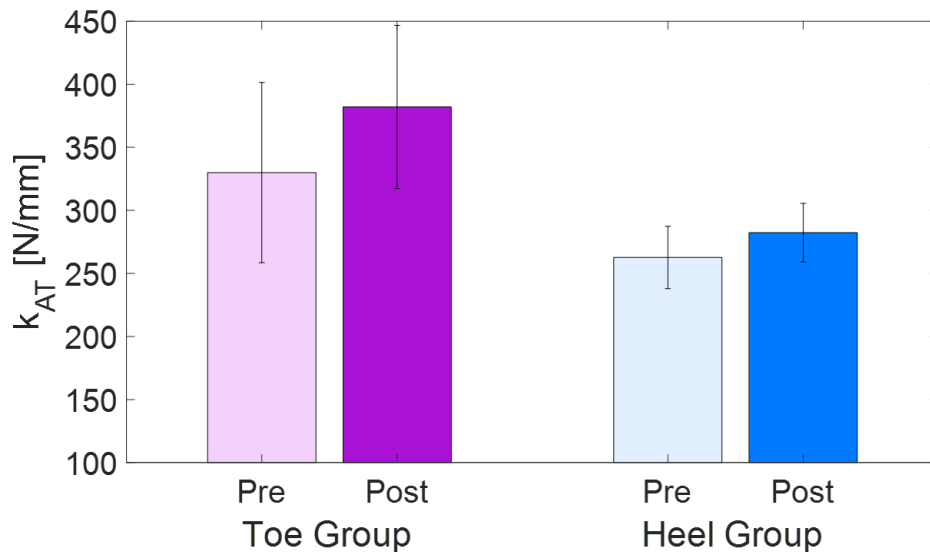
Figure 3: Achilles tendon stiffness (k_{AT}) in N/mm for toe (purple) and heel (blue) groups, pre (light) and post (dark) intervention. Error bars are standard error.

Achilles tendon cross sectional area (CSA) did not change in the high toes group (p=0.133), while high heels decreased AT CSA by 10% pre vs. post intervention (p<0.001) (Fig. 4).
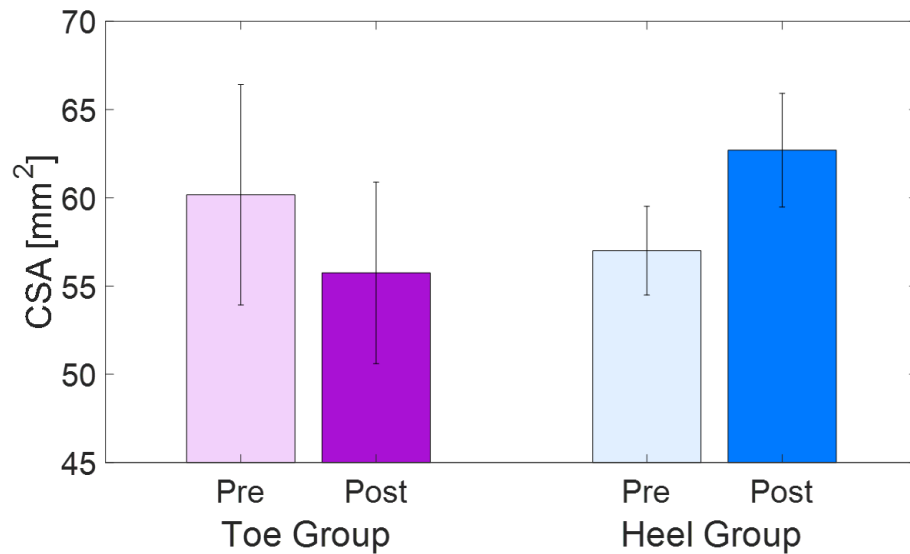
Figure 4: Achilles tendon cross sectional area (CSA) in mm^2 for toe (purple) and heel (blue) groups, pre (light) and post (dark) intervention. Error bars are standard error.

Participants varied in the number of daily steps they look in their experiment shoes. In high heels, participants took avg ± sd: 1442 ± 1257 steps/day; range: 0 to 3704 steps/day. In high toes participants took avg ± sd: 3768 ± 1626 steps/day; range: 1179 to 5998 steps/day. For every 1000 steps/day participants took in high heels their k_{AT} increased 7-

8% (β= 19 kN/m; p=0.008) (Fig. 5) and their CSA increased ~5% (β= 3 mm^2 ; p<0.001).

For every 1000 steps/day participants took in high toes their k_{AT} increased ~7% (β= 22

kN/m; p=0.019) and their CSA did not significantly change (p=0.535).
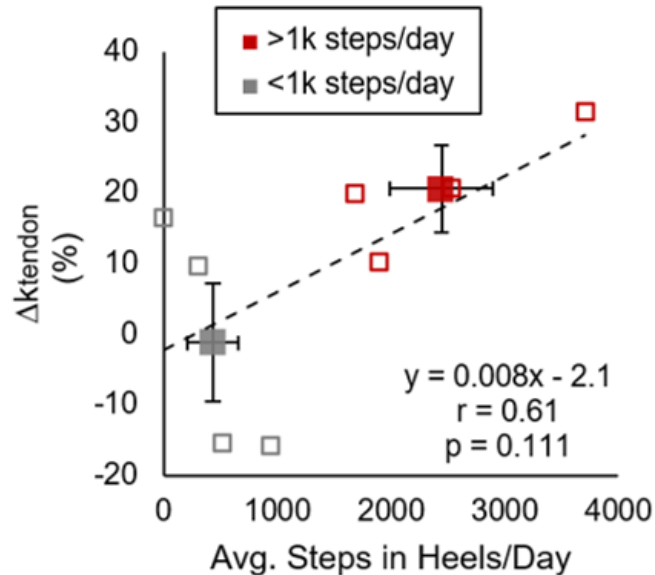
Figure 5: ΔAchilles tendon stiffness versus average steps in high heels per day over 12-16 weeks. Dashed lines indicate linear regressions on individual data (open symbols). Closed symbols represent Avg. ±SE values for participants who took >1k and <1k steps/day in high heels, respectively.

Muscle adaptation happens on a shorter times scale (~8 weeks) than tendon (~14 weeks).

To examine direction of muscle adaptation, we measured passive torque on a

dynamometer pre (0 weeks), mid (~8weeks) and post (~14 weeks) modified shoe

intervention. We found no significant different in passive torque in the toe or heel group

across time points (Fig. 6).
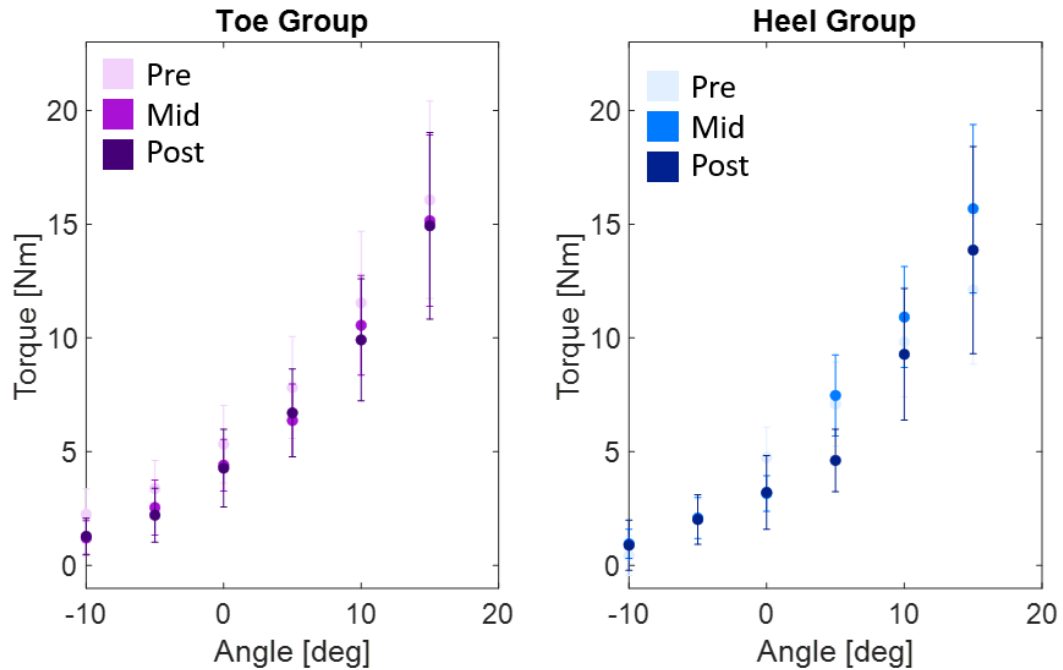
Figure 6: Passive torque at 10° PF (-10) through 15° DF ankle angle in the dynamometer for toe group (purple) and heel group (blue), at pre, mid and post 14-week intervention. Error bars are standard error.

4.4 Discussion

The purpose of this study was to investigate how relatively small changes in foot-ankle mechanics over relatively large numbers of locomotion cycles impacts muscle-tendon structure. We used modified footwear to change muscle-tendon loading and fascicle operating lengths on the triceps-surae muscle tendon unit and instructed participants to wear the shoes in their daily activities.

In the group that wore raised toes acute length of SOL and GAS fascicles at peak force increased by 10.6% (p=0.082) and 7.6% (p=0.028) respectively (Fig. 1B). In raised heels, length of SOL and GAS fascicles at peak force decreased by 18.9% (p<0.001) and 13.4% (p<0.001) respectively (Fig. 1B). Acutely, the raised toe group increased peak force on

the triceps-surae muscle tendon unit (MTU) by 8% (p<0.001) (Fig.2). Conversely, the raised heel group decreased peak force on the triceps-surae MTU by 16% (p<0.001) (Fig.2). Pre and post intervention there were not significant difference in tendon stiffness (Fig. 3) or cross-sectional area (Fig. 4). However, when accounting for the number of steps per day that each participant wore their experimental shoes, for every 1000 steps/day participants took in high heels their k_{AT} increased 7-8% (β= 19 kN/m; p=0.008) (Fig. 5) and their CSA increased ~5% (β= 3 mm^2 ; p<0.001). For every 1000 steps/day participants took in high toes their k_{AT} increased ~7% (β= 22 kN/m; p=0.019) and their CSA did not significantly change (p=0.535).

In line with our hypotheses, when accounting for steps, the tendons stiffness increased in the raised toe group, where force on the tendon was increased. Contrary to our hypothesis, even though force on the tendon we decreased acutely in the raised heel group, tendon stiffness also increased when accounting for number of cycles that participants took each day. In the raised toe group, out results are consistent with literature, where tendon stiffness increases were measure in long term protocols that increased strain (force) on tendon[43]–[45], [69]. While the increased tendon stiffness in raised heels, under conditions of decreased force was not consistent with unloading studies on the tendon[7], [117]. However, these results were consistent with studies on habitual high heel use, where increased tendon stiffness is observed[82], [84], [116]. Our torque-angle curves do not have enough resolutions for what drives the changes in tendon stiffness (Fig. 6). However, our ultrasound data indicated that our raised heel conditions significantly decreased operating lengths of both the SOL and GAS muscles (Fig. 1). Studies on muscles that are exercised at short lengths remodel to absolutely shorter by decreasing the number of sarcomeres in series[111], [112], [118]. Additionally, cross-sectional studies of high heel wearers have observed shorter calf muscle fascicle

lengths[82], [84], [116]. Our counter-intuitive tendon stiffness results for the high heel group could be due to muscles decreasing length by removing sarcomeres in series and adding strain on the tendon. This has been observed in tendon rupture repair studies where patients are placed in a plantar flexed position, similar or our high heels, and calf muscle remodel to shorter lengths while Achilles tendon stiffness increased [119], [120]. More detailed measures of muscle fascicles during a study with a protocol similar to ours can reveal the mechanism behind how both raised toes and raised heels increased tendon stiffness, when accounting for cycles.

Our results indicate that even with relatively small changes in foot-ankle mechanics, muscle-tendon structure can change if enough steps are taken over long times scales. These results are not only important for the expanding our knowledge on muscle-tendon adaption, but they also provide important insights to the wearable device field. It is important to understand the structural impact of wearing devices that modify foot-ankle mechanics long term, because musculoskeletal adaptations can alter neural activation patterns and ultimately lead to muscle-tendon units that are more or less efficient[38], [121]. Muscle tendon properties can impact whole body locomotion performance[20], [101]. Previous modeling and simulations studies suggest that muscle-tendon properties can be optimized for economical locomotion[38], [40], [41], [51]. Shorter muscle with wider CSA and stiffer tendons can enable more force production at the same excitation than their counterparts[122] and operate at more favorable conditions on the force-length relationship. In fact, when we tested participants before and after the modified shoe intervention, we found that both groups were more economical in flat shoes post intervention vs flat shoes pre intervention (Fig. 7).
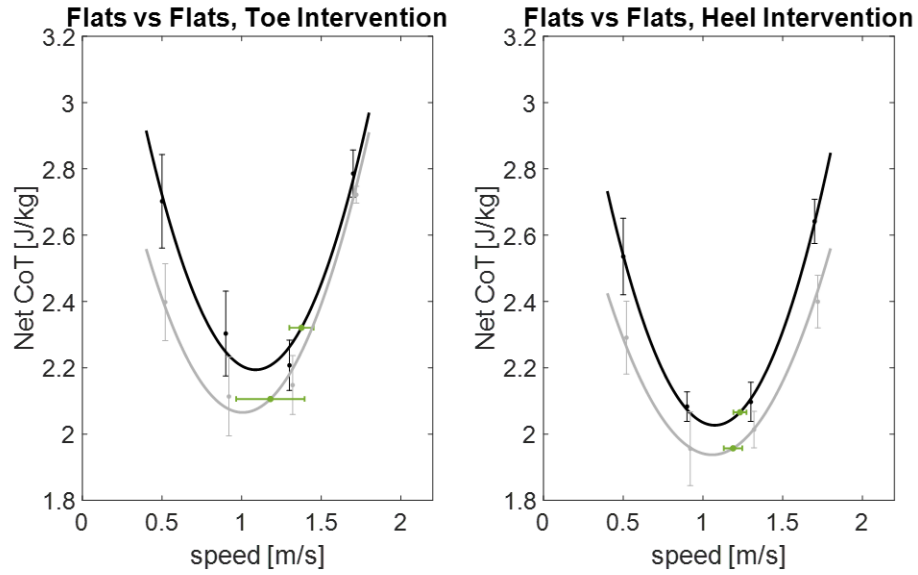
Figure 7: Metabolic cost of transport pre (black) and post (grey) intervention in flat shoes. Preferred walking speed is shown in green. Error bars are standard error.

For every 1000 steps/day that participants averaged wearing high heels, their net metabolic power during treadmill walking decreased 3% (β=-0.09 W/kg; p=0.004) (Fig. 8).
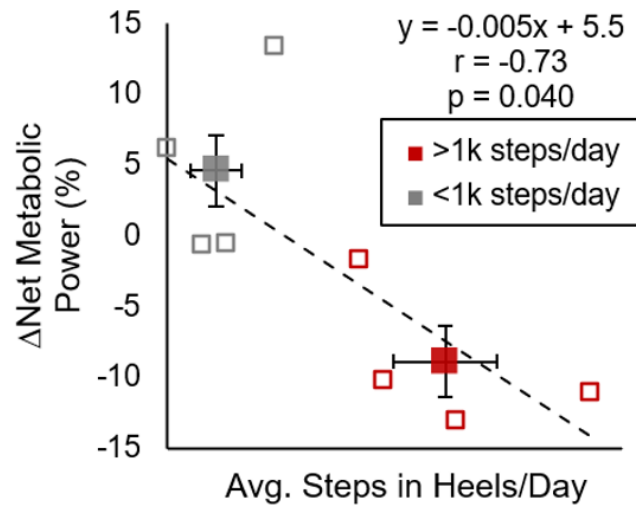
Figure 8: a) Δnet metabolic power during walking at 1.3 m/s for high heel group. Dashed lines indicate linear regressions on individual data (open symbols). Closed symbols represent Avg. ±SE values for participants who took >1k and <1k steps/day in high heels, respectively.

ΔTendon stiffness did not correlate with Δnet metabolic power during walking (r=-0.64; p=0.086) (Fig. 9). Moreover, post-hoc analyses suggest that averaging >1k steps/day in high heels is necessary to reduce net metabolic power during walking (p=0.018). Participants who averaged >1k steps/day in high heels reduced their net metabolic power during walking in flats by 9±3% (avg ± sd) (n=4; red symbols), whereas participants who averaged <1k steps/day in high heels consumed 5±7% (avg ± sd) more metabolic power during walking in flats post intervention (n=4; grey symbols) (Fig. 8).
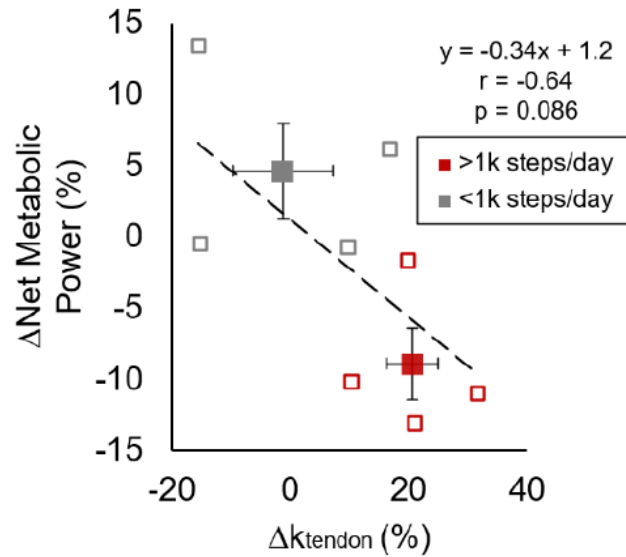
Figure 9: a) Δnet metabolic power during walking at 1.3 m/s for high heel group compared to Δktendon. Dashed lines indicate linear regressions on individual data (open symbols). Closed symbols represent Avg. ±SE values for participants who took >1k and <1k steps/day in high heels, respectively.

Despite not reaching statistical significance with 8 participants ($p=0.086$) (Fig. 9), the moderate correlation between ΔAchilles tendon stiffness and Δnet metabolic power ($r=-0.64$) supports with the notion that increasing tendon stiffness enables in-series muscles to produce force more economically [101]. Further, habitual high heel use may have also shortened calf muscle fascicles [82] and/or elicited neuromechanical changes that contributed to the improved walking economy following high heel use.

The long-term adaptions in tendon structure (increased stiffness) had functional implications as both modified shoe interventions led to improved walking economy in flat shoes pre and post intervention. The interaction between chronic structural adaptations and functional adaptions is complicated. The mechanism behind this improved economy needs to be further explored via more in depth structural measures and further gait

analysis. However, these long-term results indicate that adaption in foot-ankle

mechanics via wearable devices is both structural and functional.

CHAPTER 5
CONCLUSIONS AND FUTURE DIRECTIONS

5.1 Conclusions

In chapter 1, we outlined the importance of studying how structural and functional adaptations interact on short and long-time scales, in the context of devices that change foot ankle mechanics.

In chapter 2, we investigated how long-term use of elastic ankle exoskeletons impact Achilles tendon stiffness via a computational model. We showed that long-term use of elastic ankle exoskeletons need not reduce tendon stiffness. We demonstrated a novel computational paradigm that can inform device design and control. These results suggest that long term protection of the musculoskeletal system can be achieved in assistive devices. Additionally, this chapter suggests that a new category of wearable devices can emerge that are designed and controlled to 'steer' tissue properties.

In chapter 3, we investigated how acute changes in foot-ankle mechanics impacts locomotion performance. We found that force demand and force potential can trade off in using devices that alter foot-ankle mechanics. Despite improving force potential via shifts to longer, more optimal lengths, raised toes had no impact on force economy of the calf muscle-tendon unit, due to an increase in force demand. Raised heels decreased force demand on the calf muscle tendon unit but decreased force potential via shifter to shorter, less optimal lengths. We found that changes in foot-ankle force economy do not always reflect whole body metabolic energy expenditure.

Finally in chapter 4, we investigated the Achilles Tendon structural adaptation to long-term changes in foot-ankle mechanics. We found that the mechanobiological

response of tendons is sensitive to small changes in strain under conditions with a high number of cycles. These results demonstrate the wearable devices can modify muscle-tendon structure over long-time scales if enough steps are taken per day. Additionally, these changes in structure correlate with improved walking economy, if participants took enough steps per day in their modified shoes.

5.2 Future Directions

The body of this work can inform future directions in several fields in the context of both basic and translational questions and applications.

For those who study tissue mechano-biological response, our results suggest that Achilles tendon stiffness and cross-sectional area can be sensitive to small changes in loading, over long-time scales if enough loading cycles occur. Previous work in this field suggests that tendons will not respond to small changes in strain. Future work should explore the mechanism to these structural changes in the context of small changes in loading, and a large number of cycles. Additionally, results found increased tendon stiffness in the heels participants who took enough steps per day in their shoes. While these results are consistent with habitual high heel literature, this was in contradiction to our hypothesis that decreased strain on the tendon (via decreased calf muscle tendon unit force during walking) would lead to decreased tendon stiffness. Remodeling of tissues is a complicated process that is not just due to one factor. Future work should dive deeper in the mechanism that causes these structural changes. Collaborations between cellular level, tissue level, and in-vivo investigations are necessary to improve our understanding of tissue remodeling in the context of daily activities.

For those who design or control wearable devices, our results suggest that long term use of devices that change foot-ankle mechanics have both structural and functional impacts on the users. It is important for this field to consider these adaptations when designing, controlling, or prescribing exoskeletons. One of the primary outcome measures for this field to date has been metabolic cost reductions. For researchers with this outcome in mind, future directions should consider how economy of the user changes overtime as structure and function interact. Additionally, we showed that devices that alter foot ankle mechanics can be used as a research tool to understand on structure and function interact in the context of daily activities. We encourage the wearable robotics and device field to collaborate with biomechanists and physiologists to progress our knowledge of both how devices impact locomotion performance long term and, more basically the complicated interaction between structure and function. Finally, the body of this work can inform a new type of device in the wearables field. One that is specifically designed, controlled, or prescribed to steer tissue adaptation over long time scales. This opens new possibilities for future directions in designing and controlling devices that improve human locomotion.

Finally, for those that study human performance or exercise sciences, the results from this body of work can inform protocols that can optimize movement for targeted audiences. For example, athletes that would benefit from improvements in economy could undergo specific training protocols that target Achilles tendon stiffness. Improving our knowledge in how structure and function interact on acute and long-term time scales has direct implications for human performance. Future directions of controlled changes in structure with explicit functional outcome measures in mind can improve our knowledge in this field to improve human locomotion via training and conditioning.

REFERENCES

[1]   M. Srinivasan and A. Ruina, "Computer optimization of a minimal biped model discovers walking and running," vol. 439, no. January, 2006, doi: 10.1038/nature04113.

[2]   J. C. Selinger, J. D. Wong, S. N. Simha, and J. M. Donelan, "How humans initiate energy optimization and converge on their optimal gaits," *J. Exp. Biol.*, vol. 222, no. 19, 2019, doi: 10.1242/jeb.198234.

[3]   J. C. Selinger, S. M. O'Connor, J. D. Wong, and J. M. Donelan, "Humans Can Continuously Optimize Energetic Cost during Walking," *Curr. Biol.*, vol. 25, no. 18, pp. 2452–2456, 2015, doi: 10.1016/j.cub.2015.08.016.

[4]   M. V. Franchi *et al.*, "Architectural, functional and molecular responses to concentric and eccentric loading in human skeletal muscle," *Acta Physiol.*, vol. 210, no. 3, pp. 642–654, 2014, doi: 10.1111/apha.12225.

[5]   M. V. Franchi, N. D. Reeves, and M. V. Narici, "Skeletal muscle remodeling in response to eccentric vs. concentric loading: Morphological, molecular, and metabolic adaptations," *Front. Physiol.*, vol. 8, no. JUL, pp. 1–16, 2017, doi: 10.3389/fphys.2017.00447.

[6]   K. M. Khan and A. Scott, "Mechanotherapy: How physical therapists' prescription of exercise promotes tissue repair," *Br. J. Sports Med.*, vol. 43, no. 4, pp. 247–252, 2009, doi: 10.1136/bjsm.2008.054239.

[7]   N. D. Reeves, C. N. Maganaris, G. Ferretti, and M. V. Narici, "Influence of 90-day simulated microgravity on human tendon mechanical properties and the effect of resistive countermeasures," *J. Appl. Physiol.*, vol. 98, no. 6, pp. 2278–2286, 2005, doi: 10.1152/japplphysiol.01266.2004.

[8]   M. V. Narici, C. N. Maganaris, and N. Reeves, "Muscle and tendon adaptations to ageing and spaceflight," in *European Space Agency, (Special Publication) ESA*

SP, 2002, no. 501, pp. 69–70.

[9]   G. Epro *et al.*, "The Achilles tendon is mechanosensitive in older adults: adaptations following 14 weeks versus 1.5 years of cyclic strain exercise," *J. Exp. Biol.*, vol. 220, no. 6, pp. 1008–1018, 2017, doi: 10.1242/jeb.146407.

[10]   S. L. Lazarczuk *et al.*, "Mechanical, Material and Morphological Adaptations of Healthy Lower Limb Tendons to Mechanical Loading: A Systematic Review and Meta-Analysis," *Sport. Med.*, vol. 52, no. 10, pp. 2405–2429, 2022, doi: 10.1007/s40279-022-01695-y.

[11]   T. Wang *et al.*, "In vitro loading models for tendon mechanobiology," *J. Orthop. Res.*, vol. 36, no. 2, pp. 566–575, 2018, doi: 10.1002/jor.23752.

[12]   I. Lindemann, B. K. Coombes, K. Tucker, F. Hug, and T. J. M. Dick, "Age-related differences in gastrocnemii muscles and Achilles tendon mechanical properties in vivo," *J. Biomech.*, vol. 112, p. 110067, 2020, doi: 10.1016/j.jbiomech.2020.110067.

[13]   R. Csapo, V. Malis, J. Hodgson, and S. Sinha, "Age-related greater Achilles tendon compliance is not associated with larger plantar flexor muscle fascicle strains in senior women," *J. Appl. Physiol.*, vol. 116, no. 8, pp. 961–969, 2014, doi: 10.1152/japplphysiol.01337.2013.

[14]   C. M. Waugh, A. J. Blazevich, F. Fath, and T. Korff, "Age-related changes in mechanical properties of the Achilles tendon," *J. Anat.*, vol. 220, no. 2, pp. 144–155, 2012, doi: 10.1111/j.1469-7580.2011.01461.x.

[15]   A. Lai, G. A. Lichtwark, A. G. Schache, Y. C. Lin, N. A. T. Brown, and M. G. Pandy, "In vivo behavior of the human soleus muscle with increasing walking and running speeds," *J. Appl. Physiol.*, vol. 118, no. 10, pp. 1266–1275, 2015, doi: 10.1152/japplphysiol.00128.2015.

[16]   F. C. Anderson and M. G. Pandy, "Individual muscle contributions to support in normal walking," *Gait Posture*, vol. 17, no. 2, pp. 159–169, 2003, doi: 10.1016/S0966-6362(02)00073-5.

[17] R. R. Neptune, S. A. Kautz, and F. E. Zajac, "Contributions of the individual ankle plantar flexors to support, forward progression and swing initiation during walking," *J. Biomech.*, vol. 34, no. 11, pp. 1387–1398, 2001, doi: 10.1016/S0021-9290(01)00105-1.

[18] G. S. Sawicki, O. N. Beck, I. Kang, and A. J. Young, "The exoskeleton expansion: Improving walking and running economy," *J. Neuroeng. Rehabil.*, vol. 17, no. 1, pp. 1–9, 2020, doi: 10.1186/s12984-020-00663-9.

[19] S. H. Collins, M. Bruce Wiggin, and G. S. Sawicki, "Reducing the energy cost of human walking using an unpowered exoskeleton," *Nature*, vol. 522, no. 7555, pp. 212–215, 2015, doi: 10.1038/nature14288.

[20] R. W. Nuckols, T. J. M. Dick, O. N. Beck, and G. S. Sawicki, "Ultrasound imaging links soleus muscle neuromechanics and energetics during human walking with elastic ankle exoskeletons," *Sci. Rep.*, vol. 10, no. 1, pp. 1–15, 2020, doi: 10.1038/s41598-020-60360-4.

[21] D. P. Ferris, "The exoskeletons are here," *J. Neuroeng. Rehabil.*, vol. 6, no. 1, pp. 1–3, 2009, doi: 10.1186/1743-0003-6-17.

[22] H. Herr, "Exoskeletons and orthoses: Classification, design challenges and future directions," *J. Neuroeng. Rehabil.*, vol. 6, no. 1, pp. 1–9, 2009, doi: 10.1186/1743-0003-6-21.

[23] A. J. Young and D. P. Ferris, "State of the art and future directions for lower limb robotic exoskeletons," *IEEE Trans. Neural Syst. Rehabil. Eng.*, vol. 25, no. 2, pp. 171–182, 2017, doi: 10.1109/TNSRE.2016.2521160.

[24] D. P. Ferris, G. S. Sawicki, and M. A. Daley, "A physiologist's perspective on robotic exoskeletons for human locomotion," *Int. J. Humanoid Robot.*, vol. 4, no. 3, pp. 507–528, 2007, doi: 10.1142/S0219843607001138.

[25] S. H. Collins, M. B. Wiggin, and G. S. Sawicki, "Reducing the energy cost of human walking using an unpowered exoskeleton," *Nature*, vol. 522, no. 7555, pp. 212–215, 2015, doi: 10.1038/nature14288.

[26] P. Malcolm, W. Derave, S. Galle, and D. De Clercq, "A Simple Exoskeleton That Assists Plantarflexion Can Reduce the Metabolic Cost of Human Walking," *PLoS One*, vol. 8, no. 2, pp. 1–7, 2013, doi: 10.1371/journal.pone.0056137.

[27] L. M. Mooney and H. M. Herr, "Biomechanical walking mechanisms underlying the metabolic reduction caused by an autonomous exoskeleton," *J. Neuroeng. Rehabil.*, vol. 13, no. 1, 2016, doi: 10.1186/s12984-016-0111-3.

[28] O. N. Beck, L. K. Punith, R. W. Nuckols, and G. S. Sawicki, *Exoskeletons improve locomotion economy by reducing active muscle volume*, vol. 47, no. 4. 2019.

[29] M. J. Joyner and D. P. Casey, "Regulation of increased blood flow (Hyperemia) to muscles during exercise: A hierarchy of competing physiological needs," *Physiol. Rev.*, vol. 95, no. 2, pp. 549–601, 2015, doi: 10.1152/physrev.00035.2013.

[30] S. Bohm, F. Mersmann, A. Santuz, A. Arampatzis, and S. Bohm, "The force – length – velocity potential of the human soleus muscle is related to the energetic cost of running," 2019.

[31] D. J. Farris and G. S. Sawicki, "Human medial gastrocnemius force-velocity behavior shifts with locomotion speed and gait," *Proc. Natl. Acad. Sci.*, vol. 109, no. 3, pp. 977–982, 2012, doi: 10.1073/pnas.1107972109.

[32] E. M. Arnold, S. R. Ward, R. L. Lieber, and S. L. Delp, "A model of the lower limb for analysis of human movement," *Ann. Biomed. Eng.*, vol. 38, no. 2, pp. 269–279, 2010, doi: 10.1007/s10439-009-9852-5.

[33] L. O. F. Muscle, "The heat of shortening and the dynamic constants of muscle," pp. 136–195, 1938.

[34] R. W. Nuckols, R. W. Nuckols, R. W. Nuckols, G. S. Sawicki, and G. S. Sawicki, "Impact of elastic ankle exoskeleton stiffness on neuromechanics and energetics of human walking across multiple speeds," *J. Neuroeng. Rehabil.*, vol. 17, no. 1, pp. 1–19, 2020, doi: 10.1186/s12984-020-00703-4.

[35] O. N. Beck, L. K. Punith, R. W. Nuckols, and G. S. Sawicki, "Exoskeletons improve locomotion economy by reducing active muscle volume," *Exerc. Sport*

Sci. Rev., vol. 47, no. 4, pp. 237–245, 2019, doi: 10.1249/JES.0000000000000204.

[36] O. R. Seynnes, C. N. Maganaris, M. D. De Boer, P. E. Di Prampero, and M. V. Narici, "Early structural adaptations to unloading in the human calf muscles," *Acta Physiol.*, vol. 193, no. 3, pp. 265–274, 2008, doi: 10.1111/j.1748-1716.2008.01842.x.

[37] M. V. Narici and C. N. Maganaris, "Plasticity of the Muscle-Tendon Complex With Disuse and Aging," *Exerc. Sport Sci. Rev.*, pp. 126–134, 2007, doi: 10.1097/jes.0b013e3180a030ec.

[38] G. A. Lichtwark and A. M. Wilson, "Optimal muscle fascicle length and tendon stiffness for maximising gastrocnemius efficiency during human walking and running," vol. 252, pp. 662–673, 2008, doi: 10.1016/j.jtbi.2008.01.018.

[39] D. R. Carrier, C. Anders, and N. Schilling, "The musculoskeletal system of humans is not tuned to maximize the economy of locomotion," *Proc. Natl. Acad. Sci. U. S. A.*, vol. 108, no. 46, pp. 18631–18636, 2011, doi: 10.1073/pnas.1105277108.

[40] A. Wilson and G. Lichtwark, "The anatomical arrangement of muscle and tendon enhances limb versatility and locomotor performance," *Philos. Trans. R. Soc. B Biol. Sci.*, vol. 366, no. 1570, pp. 1540–1553, 2011, doi: 10.1098/rstb.2010.0361.

[41] T. K. Uchida, J. L. Hicks, C. L. Dembia, and S. L. Delp, "Stretching your energetic budget: How tendon compliance affects the metabolic cost of running," *PLoS One*, vol. 11, no. 3, pp. 1–19, 2016, doi: 10.1371/journal.pone.0150378.

[42] S. L. Woo, M. A. Gomez, D. Amiel, M. A. Ritter, R. H. Gelberman, and W. H. Akeson, "The effects of exercise on the biomechanical and biochemical properties of swine digital flexor tendons.," *J. Biomech. Eng.*, vol. 103, no. 1, pp. 51–56, 1981, doi: 10.1115/1.3138246.

[43] A. Arampatzis, K. Karamanidis, and K. Albracht, "Adaptational responses of the human Achilles tendon by modulation of the applied cyclic strain magnitude," *J. Exp. Biol.*, vol. 210, no. 15, pp. 2743–2753, 2007, doi: 10.1242/jeb.003814.

[44]   A. Arampatzis, A. Peper, S. Bierbaum, and K. Albracht, "Plasticity of human Achilles tendon mechanical and morphological properties in response to cyclic strain," *J. Biomech.*, vol. 43, no. 16, pp. 3073–3079, 2010, doi: 10.1016/j.jbiomech.2010.08.014.

[45]   S. Bohm, F. Mersmann, M. Tettke, M. Kraft, and A. Arampatzis, "Human Achilles tendon plasticity in response to cyclic strain: effect of rate and duration," *J. Exp. Biol.*, vol. 217, no. 22, pp. 4010–4017, 2014, doi: 10.1242/jeb.112268.

[46]   K. Karamanidis and A. Arampatzis, "Mechanical and morphological properties of different muscle-tendon units in the lower extremity and running mechanics: Effect of aging and physical activity," *J. Exp. Biol.*, vol. 208, no. 20, pp. 3907–3923, 2005, doi: 10.1242/jeb.01830.

[47]   S. Bohm, F. Mersmann, and A. Arampatzis, "Human tendon adaptation in response to mechanical loading: a systematic review and meta-analysis of exercise intervention studies on healthy adults," *Sport. Med. - Open*, vol. 1, no. 1, p. 7, 2015, doi: 10.1186/s40798-015-0009-9.

[48]   H. P. Wiesinger, A. Kösters, E. Müller, and O. R. Seynnes, "Effects of Increased Loading on in Vivo Tendon Properties: A Systematic Review," *Med. Sci. Sports Exerc.*, vol. 47, no. 9, pp. 1885–1895, 2015, doi: 10.1249/MSS.0000000000000603.

[49]   D. J. Farris and G. S. Sawicki, "Linking the mechanics and energetics of hopping with elastic ankle exoskeletons," *J. Appl. Physiol.*, vol. 113, no. 12, pp. 1862–1872, 2012, doi: 10.1152/japplphysiol.00802.2012.

[50]   D. B. Kowalsky, J. R. Rebula, L. V Ojeda, P. G. Adamczyk, and D. K. Id, "Human walking in the real world : Interactions between terrain type , gait parameters , and energy expenditure," pp. 1–14, 2021, doi: 10.1371/journal.pone.0228682.

[51]   J. Martin *et al.*, "Gauging force by tapping tendons," *Nat. Commun.*, no. 2018, pp. 2–10, 2017, doi: 10.1038/s41467-018-03797-6.

[52]   S. L. Delp *et al.*, "OpenSim : Open-Source Software to Create and Analyze Dynamic Simulations of Movement," vol. 54, no. 11, pp. 1940–1950, 2007.

[53] B. D. Robertson, D. J. Farris, and G. S. Sawicki, "More is not always better: Modeling the effects of elastic exoskeleton compliance on underlying ankle muscle-tendon dynamics," *Bioinspiration and Biomimetics*, vol. 9, no. 4, 2014, doi: 10.1088/1748-3182/9/4/046018.

[54] G. S. Sawicki and N. S. Khan, "A simple model to estimate plantarflexor muscle - tendon mechanics and energetics during walking with elastic ankle exoskeletons," 2015.

[55] T. A. L. Wren, G. S. Beaupré, and D. R. Carter, "A model for loading-dependent growth, development, and adaptation of tendons and ligaments," *J. Biomech.*, vol. 31, no. 2, pp. 107–114, 1997, doi: 10.1016/S0021-9290(97)00120-6.

[56] S. R. Young, B. Gardiner, A. Mehdizadeh, J. Rubenson, B. Umberger, and D. W. Smith, "Adaptive Remodeling of Achilles Tendon: A Multi-scale Computational Model," *PLoS Comput. Biol.*, vol. 12, no. 9, pp. 1–30, 2016, doi: 10.1371/journal.pcbi.1005106.

[57] B. D. Robertson and G. S. Sawicki, "Exploiting elasticity: Modeling the influence of neural control on mechanics and energetics of ankle muscle-tendons during human hopping," *J. Theor. Biol.*, vol. 353, pp. 121–132, 2014, doi: 10.1016/j.jtbi.2014.03.010.

[58] D. J. Farris, B. D. Robertson, and G. S. Sawicki, "Elastic ankle exoskeletons reduce soleus muscle force but not work in human hopping," *J. Appl. Physiol.*, vol. 115, no. 5, pp. 579–585, 2013, doi: 10.1152/japplphysiol.00253.2013.

[59] R. L. Lieber, "Relationship Between Achilles Tendon Mechanical Properties and Gastrocnemius Muscle Function," vol. 115, no. AUGUST, 1993.

[60] D. L. Morgan and D. G. Allen, "invited review," pp. 2007–2015, 2023.

[61] B. R. Umberger and P. E. Martin, "Mechanical power and efficiency of level walking with different stride rates," pp. 3255–3265, 2007, doi: 10.1242/jeb.000950.

[62] H. J. Ralston, "Energy-speed relation and optimal speed during level walking," *Int.*

Zeitschrift für Angew. Physiol. Einschl. Arbeitsphysiologie, vol. 17, no. 4, pp. 277–283, 1958, doi: 10.1007/BF00698754.

[63] M. Y. Zarrugh, F. N. Todd, and H. J. Ralston, "Optimization of energy expenditure during level walking," *Eur. J. Appl. Physiol. Occup. Physiol.*, vol. 33, no. 4, pp. 293–306, 1974, doi: 10.1007/BF00430237.

[64] A. E. Minetti, L. P. Ardigò, and F. Saibene, "Mechanical determinants of gradient walking energetics in man.," *J. Physiol.*, vol. 472, no. 1, pp. 725–735, 1993, doi: 10.1113/jphysiol.1993.sp019969.

[65] J. M. Donelan, R. Kram, and A. D. Kuo, "Mechanical and metabolic determinants of the preferred step width in human walking," *Proc. R. Soc. B Biol. Sci.*, vol. 268, no. 1480, pp. 1985–1992, 2001, doi: 10.1098/rspb.2001.1761.

[66] R. M. Alexander, "Optimum Muscle Design for Oscillatory Movements," *J. Theor. Biol.*, no. August 1996, pp. 253–259, 1997.

[67] T. Althoff, J. L. Hicks, A. C. King, S. L. Delp, Z. Biohub, and S. Francisco, "Large-scale physical activity data reveal worldwide activity inequality," vol. 547, no. 7663, pp. 336–339, 2018, doi: 10.1038/nature23018.Large-scale.

[68] T. Wang *et al.*, "Programmable mechanical stimulation influences tendon homeostasis in a bioreactor system," *Biotechnol. Bioeng.*, vol. 110, no. 5, pp. 1495–1507, 2013, doi: 10.1002/bit.24809.

[69] A. Arampatzis, A. Peper, S. Bierbaum, and K. Albracht, "Plasticity of human Achilles tendon mechanical and morphological properties in response to cyclic strain," *J. Biomech.*, vol. 43, no. 16, pp. 3073–3079, 2010, doi: 10.1016/j.jbiomech.2010.08.014.

[70] C. Mccrum *et al.*, "Loading rate and contraction duration effects on in vivo human Achilles tendon mechanical properties," *Clin. Physiol. Funct. Imaging*, pp. 1–7, 2017, doi: 10.1111/cpf.12472.

[71] M. Kharazi, S. Bohm, C. Theodorakis, F. Mersmann, and A. Arampatzis, "Quantifying mechanical loading and elastic strain energy of the human Achilles

tendon during walking and running," *Sci. Rep.*, vol. 11, no. 1, pp. 1–13, 2021, doi: 10.1038/s41598-021-84847-w.

[72]   A. Arampatzis, K. Karamanidis, L. Mademli, and K. Albracht, "Plasticity of the Human Tendon to Short- and Long-Term Mechanical Loading," 2009.

[73]   D. J. Farris, B. D. Robertson, and G. S. Sawicki, "Elastic ankle exoskeletons reduce soleus muscle force but not work in human hopping," *J. Appl. Physiol.*, vol. 115, no. 5, pp. 579–585, 2013, doi: 10.1152/japplphysiol.00253.2013.

[74]   A. M. Grabowski and H. M. Herr, "Leg exoskeleton reduces the metabolic cost of human hopping," *J. Appl. Physiol.*, vol. 107, no. 3, pp. 670–678, 2009, doi: 10.1152/japplphysiol.91609.2008.

[75]   K. Kubo *et al.*, "Effects of plyometric and weight training on muscle-tendon complex and jump performance," *Med. Sci. Sports Exerc.*, vol. 39, no. 10, pp. 1801–1810, 2007, doi: 10.1249/mss.0b013e31813e630a.

[76]   D. J. Farris and G. S. Sawicki, "The mechanics and energetics of human walking and running : a joint level perspective," no. May 2011, pp. 110–118, 2012.

[77]   T. A. L. Wren, G. S. Beaupré, and D. R. Carter, "A model for loading-dependent growth, development, and adaptation of tendons and ligaments," *J. Biomech.*, vol. 31, no. 2, pp. 107–114, 1997, doi: 10.1016/S0021-9290(97)00120-6.

[78]   G. S. Sawicki and D. P. Ferris, "Mechanics and energetics of level walking with powered ankle exoskeletons," *J. Exp. Biol.*, vol. 211, no. 9, pp. 1402–1413, 2008, doi: 10.1242/jeb.009241.

[79]   C. Ebbeling and A. Crussemeyer, "Lower Extremity Mechanics and Energy Cost of Walking in High-Heeled Shoes," vol. 19, no. 4, 1994.

[80]   P. Antonellis, C. M. Frederick, A. M. Gonabadi, and P. Malcolm, "Modular footwear that partially offsets downhill or uphill grades minimizes the metabolic cost of human walking," *R. Soc. Open Sci.*, vol. 7, no. 2, 2020, doi: 10.1098/rsos.191527.

[81] J. X. Li, Y. Hong, and D. Mao, "Gait and the Metabolic Adaptation of Walking with Negative Heel Shoes," *Res. Sport. Med.*, vol. 11, no. 4, pp. 277–296, 2003, doi: 10.1080/714041041.

[82] R. Csapo, C. N. Maganaris, O. R. Seynnes, and M. V Narici, "On muscle , tendon and high heels," pp. 2582–2588, 2010, doi: 10.1242/jeb.044271.

[83] K. E. Gordon and D. P. Ferris, "Learning to walk with a robotic ankle exoskeleton," *J. Biomech.*, vol. 40, no. 12, pp. 2636–2644, 2007, doi: 10.1016/j.jbiomech.2006.12.006.

[84] N. J. Cronin, "The effects of high heeled shoes on female gait: A review," *J. Electromyogr. Kinesiol.*, vol. 24, no. 2, pp. 258–263, 2014, doi: 10.1016/j.jelekin.2014.01.004.

[85] D. J. Stefanyshyn, B. M. Nigg, V. Fisher, B. O'Flynn, and W. Liu, "The influence of high heeled shoes on kinematics, kinetics, and muscle EMG of normal female gait," *J. Appl. Biomech.*, vol. 16, no. 3, pp. 309–319, 2000, doi: 10.1123/jab.16.3.309.

[86] E. B. Simonsen *et al.*, "Walking on high heels changes muscle activity and the dynamics of human walking significantly," *J. Appl. Biomech.*, vol. 28, no. 1, pp. 20–28, 2012, doi: 10.1123/jab.28.1.20.

[87] R. G. Ellis, B. J. Sumner, and R. Kram, "Muscle contributions to propulsion and braking during walking and running: Insight from external force perturbations," *Gait Posture*, vol. 40, no. 4, pp. 594–599, 2014, doi: 10.1016/j.gaitpost.2014.07.002.

[88] O. N. Beck, L. H. Trejo, J. N. Schroeder, J. R. Franz, and G. S. Sawicki, "Shorter muscle fascicle operating lengths increase the metabolic cost of cyclic force production," *J. Appl. Physiol.*, vol. 133, no. 3, pp. 524–533, 2022, doi: 10.1152/japplphysiol.00720.2021.

[89] J.-S. L. Kim and Hae-dong, "Acute Changes in Fascicle Behavior and Electromyographic Activity of the Medial Gastrocnemius during Walking in High Heeled Shoes," vol. 26, no. 1, pp. 135–142, 2016.

[90] M. D. Péronnet F, "Table of nonprotein respiratory quotient : an update .," *Can J Sport Sci*, no. November, pp. 23–29, 1991.

[91] D. J. Farris and G. A. Lichtwark, "UltraTrack: Software for semi-automated tracking of muscle fascicles in sequences of B-mode ultrasound images," *Comput. Methods Programs Biomed.*, vol. 128, pp. 111–118, 2016, doi: 10.1016/j.cmpb.2016.02.016.

[92] G. G. Hands, C. H. Meyer, J. M. Hart, M. F. Abel, and S. S. Blemker, "Relationships of 35 lower limb muscles to height and body mass quanti fi ed using MRI," vol. 47, pp. 631–638, 2014, doi: 10.1016/j.jbiomech.2013.12.002.

[93] E. M. Arnold, S. R. Hamner, A. Seth, M. Millard, and S. L. Delp, "How muscle fiber lengths and velocities affect muscle force generation as humans walk and run at different speeds," *J. Exp. Biol.*, vol. 216, no. 11, pp. 2150–2160, 2013, doi: 10.1242/jeb.075697.

[94] A. K. Perry, R. Blickhan, A. A. Biewener, N. C. Heglund, and C. R. Taylor, "Preferred speeds in terrestrial vertebrates: are they equivalent?," *J. Exp. Biol.*, vol. 137, pp. 207–219, 1988, doi: 10.1242/jeb.137.1.207.

[95] V. R. Edgerton and J. L. Smith, "Muscle fibre type populations of human leg muscles," vol. 7, pp. 259–266.

[96] J. Rubenson, N. J. Pires, H. O. Loi, G. J. Pinniger, and D. G. Shannon, "On the ascent : the soleus operating length is conserved to the ascending limb of the force – length curve across gait mechanics in humans," pp. 3539–3551, 2012, doi: 10.1242/jeb.070466.

[97] D. F. B. Haeufle, S. Grimmer, and A. Seyfarth, "The role of intrinsic muscle properties for stable hopping - Stability is achieved by the force-velocity relation," *Bioinspiration and Biomimetics*, vol. 5, no. 1, 2010, doi: 10.1088/1748-3182/5/1/016004.

[98] N. Waterval, J. Harlaar, F. Nollet, and M. Brehm, "Gait & Posture Compensatory gait strategies for reduced ankle work in patients with unilateral fl accid calf muscle weakness," *Gait Posture*, vol. 57, p. 27, 2017, doi:

10.1016/j.gaitpost.2017.07.021.

[99]   D. J. Farris, A. Hampton, M. D. Lewek, and G. S. Sawicki, "Revisiting the mechanics and energetics of walking in individuals with chronic hemiparesis following stroke : from individual limbs to lower limb joints," pp. 1–12, 2015, doi: 10.1186/s12984-015-0012-x.

[100] P. Malcolm, R. E. Quesada, J. M. Caputo, and S. H. Collins, "The influence of push-off timing in a robotic ankle-foot prosthesis on the energetics and mechanics of walking," *J. Neuroeng. Rehabil.*, vol. 12, no. 1, 2015, doi: 10.1186/s12984-015-0014-8.

[101] R. L. Krupenevich, O. N. Beck, G. S. Sawicki, and J. R. Franz, "Reduced Achilles Tendon Stiffness Disrupts Calf Muscle Neuromechanics in Elderly Gait," *Gerontology*, vol. 68, no. 3, pp. 241–251, 2022, doi: 10.1159/000516910.

[102] P. E. Dvita, T. Hortobagyi, and N. Carolina, "Age causes a redistribution of joint torques and powers during gait," pp. 1804–1811, 2023.

[103] D. C. Kerrigan *et al.*, "Biomechanical Gait Alterations Independent of Speed in the Healthy Elderly : Evidence for Specific Limiting Impairments "! X ,/," no. March, pp. 317–322, 1998.

[104] O. N. Beck, L. H. Trejo, J. N. Schroeder, J. R. Franz, and G. S. Sawicki, "Shorter Muscle Fascicle Operating Lengths Increase the Metabolic Cost of Cyclic Force Production," *J. Appl. Physiol.*, no. 8.5.2017, pp. 2003–2005, 2022.

[105] A. Monte, P. Tecchio, F. Nardello, L. P. Ardigò, P. Zamparo, and B. Bachero-mena, "The interplay between gastrocnemius medialis force – length and force – velocity potentials , cumulative EMG activity and energy cost at speeds above and below the walk to run transition speed," no. October 2022, pp. 90–102, 2023, doi: 10.1113/EP090657.

[106] A. D. Christie, S. A. Foulis, and J. A. Kent, "ATP cost of muscle contraction is associated with motor unit discharge rate in humans," *Neurosci. Lett.*, vol. 629, pp. 186–188, 2016, doi: 10.1016/j.neulet.2016.07.007.

[107] B. R. Umberger, K. G. M. Gerritsen, and P. E. Martin, "A model of human muscle energy expenditure.," *Comput. Methods Biomech. Biomed. Engin.*, vol. 6, no. 2, pp. 99–111, 2003, doi: 10.1080/1025584031000091678.

[108] B. R. Umberger and J. Rubenson, "Understanding muscle energetics in locomotion: New modeling and experimental approaches," *Exerc. Sport Sci. Rev.*, vol. 39, no. 2, pp. 59–67, 2011, doi: 10.1097/JES.0b013e31820d7bc5.

[109] R. L. Lieber and S. R. Ward, "Skeletal muscle design to meet functional demands," *Philos. Trans. R. Soc. B Biol. Sci.*, vol. 366, no. 1570, pp. 1466–1476, 2011, doi: 10.1098/rstb.2010.0316.

[110] A. Hinks, M. V. Franchi, and G. A. Power, "The influence of longitudinal muscle fascicle growth on mechanical function," *J. Appl. Physiol.*, vol. 133, no. 1, pp. 87–103, 2022, doi: 10.1152/japplphysiol.00114.2022.

[111] A. Hinks, B. Davidson, and G. A. Power, "Influence of isometric training at short and long muscle-tendon unit lengths on the history dependence of force," no. May 2020, pp. 325–338, 2021, doi: 10.1111/sms.13842.

[112] A. M. Zöllner, J. M. Pok, E. J. McWalter, and G. E. Gold, "On high heels and short muscles: A multiscale model for sarcomere loss in the gastrocnemius muscle," pp. 301–310, 2016, doi: 10.1016/j.jtbi.2014.10.036.On.

[113] S. P. Magnusson, M. V. Narici, C. N. Maganaris, and M. Kjaer, "Human tendon behaviour and adaptation, in vivo," *J. Physiol.*, vol. 586, no. 1, pp. 71–81, 2008, doi: 10.1113/jphysiol.2007.139105.

[114] M. V. Narici, C. N. Maganaris, and N. D. Reeves, "Myotendinous alterations and effects of resistive loading in old age," *Scand. J. Med. Sci. Sport.*, vol. 15, no. 6, pp. 392–401, 2005, doi: 10.1111/j.1600-0838.2005.00458.x.

[115] G. Mcmahon and G. Mcmahon, "No Strain , No Gain ? The Role of Strain and Load Magnitude in Human Tendon Responses and Adaptation to Loading," no. July, 2022, doi: 10.1519/JSC.0000000000004.

[116] N. J. Cronin, R. S. Barrett, and C. P. Carty, "Long-term use of high-heeled shoes

alters the neuromechanics of human walking," *J. Appl. Physiol.*, vol. 112, no. 6, pp. 1054–1058, 2012, doi: 10.1152/japplphysiol.01402.2011.

[117] D. Shin *et al.*, "Effect of chronic unloading and rehabilitation on human Achilles tendon properties: a velocity-encoded phase-contrast MRI study," *J. Appl. Physiol.*, 2008, doi: 10.1152/japplphysiol.90699.2008.

[118] A. Hinks, M. Franchi, and G. Power, "The influence of longitudinal muscle fascicle growth on mechanical function," pp. 95–100, 2022.

[119] B. Stäudle, O. Seynnes, G. Laps, G. P. Brüggemann, and K. Albracht, "Altered Gastrocnemius Contractile Behavior in Former Achilles Tendon Rupture Patients During Walking," *Front. Physiol.*, vol. 13, no. March, pp. 1–12, 2022, doi: 10.3389/fphys.2022.792576.

[120] B. Stäudle, O. Seynnes, G. Laps, F. Göll, G. P. Brüggemann, and K. Albracht, "Recovery from Achilles Tendon Repair: A Combination of Postsurgery Outcomes and Insufficient Remodeling of Muscle and Tendon," *Med. Sci. Sports Exerc.*, vol. 53, no. 7, pp. 1356–1366, 2021, doi: 10.1249/MSS.0000000000002592.

[121] G. A. Lichtwark and A. M. Wilson, "Interactions between the human gastrocnemius muscle and the Achilles tendon during incline, level and decline locomotion," *J. Exp. Biol.*, vol. 209, no. 21, pp. 4379–4388, 2006, doi: 10.1242/jeb.02434.

[122] A. A. Biewener and T. J. Roberts, "Muscle and tendon contributions to force, work, and elastic energy savings: A comparative perspective," *Exerc. Sport Sci. Rev.*, vol. 28, no. 3, pp. 99–107, 2000.